1 wp

NASA TECHNICAL TRANSLATION NASA TT F-14,237

RELIABILITY OF CONVERTER NETWORKS OF THERMIONIC POWER SUPPLY EQUIPMENTS

S. Dagbjartsson

Translation of: "Zuverlässgkeit der Konverternetzwerke von thermionischen Energieversorgungsanlagen", Stuttgart, Universitat, Inst. fur Kernenergetik, 1970, 72 pages.

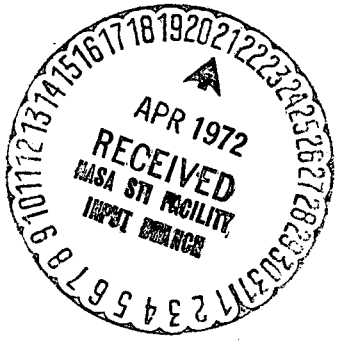

NATIONAL AERONAUTICS AND SPACE ADMINISTRATION
WASHINGTON, D. C. 20546 APRIL 1972

CAT. 10

TABLE OF CONTENTS

Explanation of symbols

Abbreviations

A: Richardson constant, 120 A/cm^2K^2 in Eq. (2.1).
Otherwise, the number of failed converters in a network.
c: Energy liberated per nuclear fission (≈ 200 MeV)
d: Electrode separation ( )
E: Neutron energy (eV)
e: Elemental charge, $1.602 \cdot 10^{-19}$ A sec
f: Cross-sectional area (cm^2)
I: Converter current (A)
j: Electrical current density (A/cm^2)
K: Number of short-circuited converters
k: Boltzmann constant ($8.616 \cdot 10^{-5}$ eV/K)
L: Number of converters failed during idling
l: Length (cm)
N: Number of converters in a network
ΔN: Power loss of a network as a result of converter failure (%)
P, p: Probability
Q: Heat flux (W)
q: Heat flux density (W/cm^2)
R: Electrical resistance (Ω)
S: Back-scattering coefficient
s: Number of parallel-connected converters in a network
T: Temperature (K)
U: Electrical potential (V)
V: Potential difference (V)
z: Number of series-connected converters in a network
α: Increase of a linearized converter characteristic
β: Current of a converter with U = 0
ε Emissivity
η: Efficiency
$\varkappa$: Thermal conductivity (W/cm K)
λ: Mean free path (μ)
ϱ: Specific electrical resistance (Ω cm)

/6

σ : Stefan-Boltzmann constant ($W/cm^2\ K^4$)

$\Sigma_{(\nu,E)}$: Macroscopic fission cross section (cm^{-1})

$\phi_{(\nu,E)}$ Neutron flux density (neutrons/cm^2 sec)

ϕ : Exit potential (V)

φ : Potential of a node point in the converter network

$\mathfrak{Q}$: Heat supply (W)

ϖ : Mean heat supply density (W/cm^3)

Indices

A: Failure

C: Collector

E: Emitter

el: Electrons (passing through)

i, j, k: Integral indices

K: Short circuit

L: Idling

q: Cross-connection

s: Saturation

st: Radiation (passing through)

V: Load

vs: Connecting cross-piece

z: Converter cell

ε_E: Electrons at the emitter

RELIABILITY OF CONVERTER NETWORKS OF THERMIONIC POWER SUPPLY EQUIPMENTS

S. Dagbjartsson

Taking into account the current-voltage characteristics of thermionic converters, the current and voltage values characteristic of the individual branches of a network are examined, particular attention being given to the failure of individual converters. The failure is considered to be a statistical event that occurs with equal probability in all converters during the operation of a converter network. This formalism makes it possible to calculate the network reliability as a function of the possible excess output at the beginning of the operation period. It has been found that the probability of failure of any converter is 5%, and that the emitter temperature of some converters, which is initially about 1860°K, exceeds with a probability of about 10% the temperature of 2000°K.

1. INTRODUCTION

Nuclear reactors are desirable for supply of electrical / 7 * power to spacecraft having power requirements above about 20 kW (Pruschek, 1968). They have a high energy content and can operate for long periods without maintenance.

In ground-based systems, the conversion of the primary heat produced in the reactor into electrical energy is done generally by means of steam turbines. But this method proves to be impractical for space conditions. First, it requires large masses, which are very expensive to transport out of the earth's gravity field. Second, large rotating parts are undesirable in satellites.

---

* Numbers in the margin indicate the pagination in the original foreign text.

Direct conversion of thermal energy into electrical energy is possible with thermoelectric as well as thermionic converters. Their use in connection with nuclear reactors has been discussed repeatedly (Höcker and co-workers, 1965). Of these two methods, thermionic energy conversion is conceded to have greater future prospects, as it has significantly higher efficiency. The high working temperature of the thermionic converter provides another advantage, because smaller radiators are required for the elimination of the waste heat (Groll, 1965). On the other hand, these high working temperatures have undesirable consequences related to the technical design of the converter. It is necessary to maintain separations of fractions of a millimeter between two electrodes, electrically insulated from each other, with temperatures of around 1,000 or 2,000°K, with a cesium pressure of a few Torr in the electrode gap. These problems have so far prevented the development of a converter having a power capacity which can be expected to last for years. But steady advances in converter lifetime have been made. For instance, prolonged experiments with flat laboratory converters in the Jet Propulsion Laboratory (USA) in 1962 gave a maximum lifetime of 119 hours, while it was 15,210 hours in 1968 (Ruklove, 1968). / 8

In the radiation field of a nuclear reactor, the converter materials are also exposed to radiation damage, which can also decrease the lifetime.

These results show that the working time of a thermionic reactor is limited by the lifetime of the converter, as other factors — such as the consumption of the nuclear fuel — allow maintenance-free operation for some years.

No uniform lifetime can be expected for all the converters of a thermionic reactor. Rather, small differences in their fabrication or loading will cause them to fail after various lengths of time, without the lifetime for any single converter

being known in advance. Thus, one can only make statistical predictions of the life expectancy of the converter. On the basis of such predictions, studies on the reliability of converter networks have been in process at the Gulf General Atomics company in the USA since 1965 (Holland, 1965). Such studies are also being performed in the Soviet Union (Diakov, 1968). But very little concrete information has been published, for security reasons.

This work is concerned with this circle of topics. It first describes the theory of converter networks. The effect of converter failures in the network, and the statistical nature of their occurrence, are discussed in another chapter. At the end of the treatment, the application of the theory which is formulated is shown with the example of the ITR partially thermionic reactor (Budnik, 1968).

2. CONVERTER NETWORKS / 9

Many converters are required to have a thermionic power supply system with a power in the kW range, as the power produced by one converter is at most a few hundreds of watts at a voltage of about 0.5 volts. The low voltage of the converter is particularly disadvantageous. In order to multiply it, several converters can be connected in series. But the possibility that the circuit will be interrupted by breakage of a connection or the idling operation of one converter argues against the series connection of all the converters of a power supply system. This danger is prevented by parallel connection of several converters. In this way we get a series-parallel network (Figure 2.1), the dimensions of which result from the requirements for the highest possible voltage and reliability with a prescribed number of converters. Section 4.2.2 describes the development of converter networks in an in-core thermionic reactor.

Kirchoff's rule

$$\Sigma I = 0 \qquad (2.1)$$

for the currents at each junction in the network is used in a calculation of the electrical data for a network of converters P (k/i) (Figure 2.1). Here the converter currents $I_{k,\,i}$ and $I_{k+1,\,i}$ of the adjacent converter are two of the currents I at the junction P(k/i). Except for the boundary points P(k/1)* or P(k/s) (k = 1, 2, . . . , z-1) into which only one cross connection discharges, in general two other currents meet at the junction P(k/i). These flow through the transverse resistances $R_{k,\,i-1}$ and $R_{k,\,i}$.

/ 10

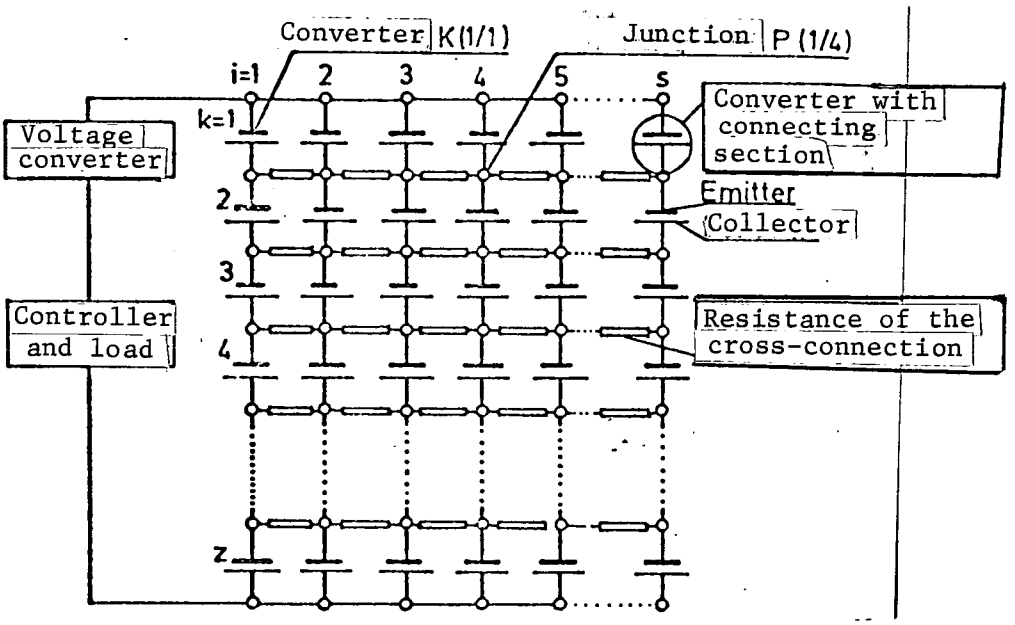

Figure 2.1. Equivalent circuit of a converter network.

*Translator's Note: 1 = one.

Ohm's law

$$R_{k,i} \cdot \bar{I}_{k,i} = \varphi_{k,i+1} - \varphi_{k,i} \qquad (2.2)$$

applies to these cross currents $\bar{I}_{k,i}$, where the potential on the cross resistance $R_{k,i}$ is expressed by the electrical potentials of the adjacent junctions.

After insertion of the expression for the cross flow from Equation (2.2), Equation (2.1) gives the following equation for the current balance at the junction P(k,i):

$$I_{k,i} - I_{k+1,i} + \frac{\varphi_{k,i} - \varphi_{k,i-1}}{R_{k,i-1}} - \frac{\varphi_{k,i+1} - \varphi_{k,i}}{R_{k,i}} = 0 \qquad (2.3)$$

A network with z converters connected in series and s in parallel (s·z network) has s(z-2) junctions, for each of which a defining equation of the form of (2.3) can be established for the current balance. The following unknowns appear in these equations:

1) s · z converter currents, $I_{k,i}$ / 11
2) s(z-1) potentials $\bar{\phi}_{k,i}$ at the junctions
3) one potential $\bar{\phi}+$ at the upper end of the network. The potential at the lower end of the network is arbitrarily set equal to zero.

In order to determine the $2 \cdot s \cdot z - s+1$ unknowns in the problem, we have available, along with the s(z-1) balance equations for the currents at the network junctions, the s·z current-voltage characteristics of the converters. They represent a functional relation between the converter current and the potential difference between the junctions for the converters in question (the converter potential)

$$I_{k,i} = f(\varphi_{k,i} - \varphi_{k-1,i}) \qquad (2.4)$$

We will investigate this relation in the following section.

The final one of these equations needed for complete definition of the problem arises from the properties of the outer part of the current loop, in which we find the load and, in general, also a voltage converter (see Figure 2.1). For calculation of the network data, an ohmic resistance R_V is assumed for this part of the circuit.

2.1 Converter Characteristics

The current-voltage characteristic of a thermionic cesium converter is affected by many parameters. These include, among others, the emitter and collecter temperatures, cesium pressure, emitter material, the surface nature of the emitter, the electrode separation, and the heat input (Rufeh, 1968). Because of the high number of parameters, an exact theoretical / 12 determination of the characteristic is extremely difficult. Rasor (1965) set up a simplified theoretical converter model which considered the most important effects in the converter and provided results sufficiently accurate for many purposes (Kondratiev, 1968). Depending on the type of the ionization process in the cesium gas in the electrode gap, we differentiate between the surface ionization region and the volume ionization region of converter operation (Figure 2.2). While practical significance can hardly be ascribed to operation of the converter in the surface ionization region (Wolf, 1968), considerable power densities can be attained in the volume ionization region (> 20 W/cm^2) at high efficiency ($> 15\%$). In this work, therefore, we assume operation of the converter in the volume ionization region.

2.1.1. Rasor converter model

According to Rasor's model concept, the current-voltage characteristic of a thermionic converter with constant emitter temperature (Figure 2.2) in the volume ionization region is given by the analytical expressions (2.5) and (2.7). Thus, for the net current density in the electrode gap, j, as a function of the converter potential in the saturation region of the characteristic we have

$$j = \frac{j_S}{1 + \exp(-(\varphi_E - \varphi_C + V_C - V)e/kT_{\ell E})(3d/4\lambda_{\ell}s)} \qquad (2.5)$$

Here j_S is the saturation current density leaving the emitter, according to the Richardson Equation

$$j_S = AT_E^2 \exp(-e\varphi_E/kT_E) \qquad (2.6)$$

It is reduced to the value j by the potential distribution in the electrode gap (see Figure 2.3) and by the scattering of the electrons in the converter plasma.

/ 13

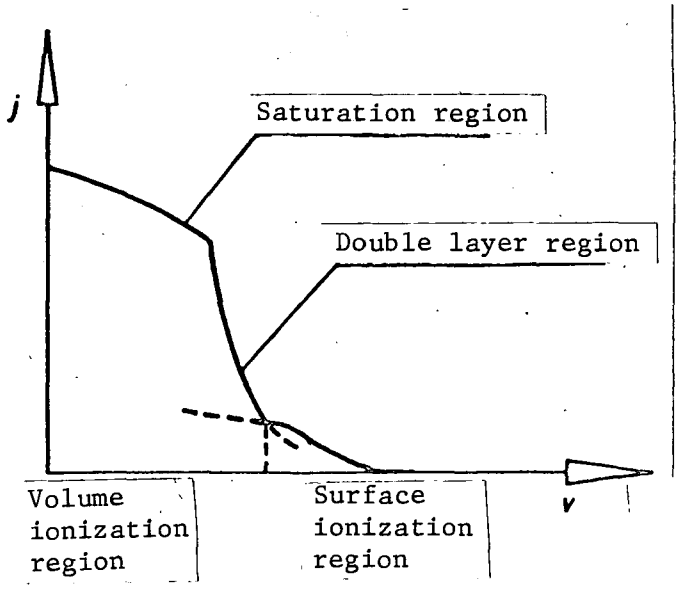

Figure 2.2: Current-voltage characteristic of a converter.

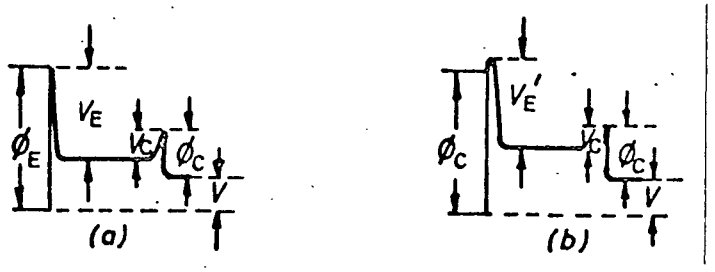

Figure 2.3: Potential curve in the saturation region (a) and in the double-layer region (b) of the current-voltage characteristic (according to Rasor).

/ 14

In the double-layer region of the characteristic, a negative space charge develops in front of the emitter (see Figure 2.3 (b)). This prevents the free exit of the electrons according to the Richardson equation. Thus, the following expression

$$j = \frac{AT_E^2 \exp(-e(V_E' - V_C - \phi_E + \phi_C)/kT_E)}{1 + \exp(eV_E'/kT_E)(3d/4\lambda + S)} \exp(-eV/kT_E) \qquad (2.7)$$

arises from Equation (2.5) for the current-voltage characteristic in the double-layer region. The theoretical derivation of Equations (2.5) and (2.7) from the assumptions applied was treated extensively by Rasor (1965).

2.1.2. Converter characteristics at constant heat input

In the converter model discussed theoretically, the heat balance in the converter does not receive primary consideration. Instead, it is assumed that the heat flux necessary to maintain the prescribed emitter temperature and the matching current density are available. In operation of a thermionic power supply

system, however, the heat input to the converter is specified, and not its emitter temperature. Thus, it is reasonable to base the network calculations on the current-voltage characteristic at prescribed (constant) heat input. These characteristics and the emitter temperatures can be calculated by means of Rasor's converter model, with consideration of the heat balance.

Various physical transport mechanisms contribute to the cooling of the emitter.

1) Electron cooling

The electrons in the emitter have a thermal energy because of their temperature. It is removed when they leave the emitter. Holland (1963) has described this energy loss / 15 from the emitter by the equation

$$q_{el} = j(V+b) \qquad (2.8)$$

In general, the empirical constant b depends only slightly on the converter operating parameters. Its numerical value is about 2.6 V.

2) Radiation cooling

The heat transport between the electrodes of a converter due to radiation is given by

$$q_{st} = \varepsilon_{EC}(T_E^4 - T_C^4) \qquad (2.9)$$

with

$$\varepsilon_{EC} = (1/\varepsilon_E + 1/\varepsilon_C - 1)^{-1} \qquad (2.10)$$

Thus, according to Schock (1968) it is based on the emissivities of the electrodes, $\overline{\varepsilon_E}$ and $\overline{\varepsilon_C}$ at the emitter temperature.

3) Heat conduction across the connecting section

To lead off the electrical energy produced in the converter, there must be a conductor (connecting section) linked with the emitter. Relatively large currents flow through this section, which is in general connected to the collector of the adjacent converter (series connection). Therefore, its dimensions must be optimized with respect to ohmic losses and the heat led away from the emitter. For a given length, the optimum cross section is given by (Wolf, 1968):

$$f_{vs} = \Pi_{vs}\sqrt{\frac{2-\eta}{2\eta}\frac{\rho_{vs}}{\kappa_{vs}(T_E-T_C)}} \qquad (2.11)$$

The amount of heat lost this way can be calculated as / 16

$$q_{vs} = f_{vs}\kappa_{vs}\frac{T_E - T_C}{l_{vs}} \qquad (2.12)$$

In general, it amounts to some 10% of the heat load on the emitter.

Other physical effects, such as heat conduction through the cesium plasma and the Joule heat produced in the connecting section, contribute only a small amount (less than 10%) to the heat balance of the converter.

Figure 2.4 shows characteristics which were calculated according to the theoretical converter model of Rasor. A constant emitter temperature was assumed for the solid curves, while for the dashed characteristics, constant heat input was assumed.

2.2 Linearization of the Network Equations

Equation (2.3) represents a linear relation between the currents in the branches of a network and the potentials at its junctions. Likewise, the characteristic for the assumed

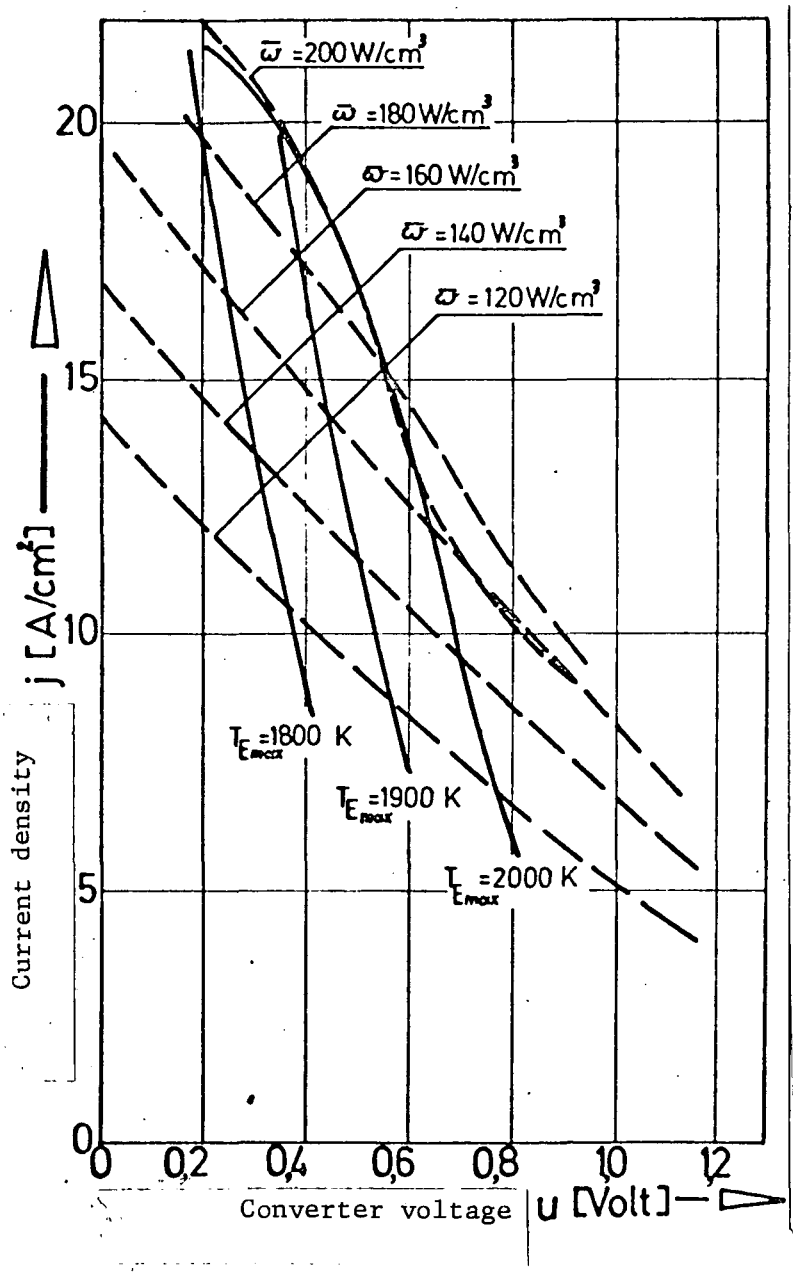

Figure 2.4: Characteristic lines for an ITR converter (calculated according to the converter model of Rasor).

load is linear. However, the current-voltage characteristics of the converter at constant heat input can be given only by implicit expressions produced by replacement of the emitter temperature in Equation (2.5) and (2.7) by the heat input from Equations (2.8), (2.9) and (2.12). In order to circumvent the resulting difficulty in the calculation of the network data, use was made of the the property of the characteristics, that, as long as the converter is operated in the double-layer region, they can be approximately reproduced by the linear relation

$$I_{k,i} = \alpha_{k,i}(\varphi_{k,i} - \varphi_{k-1,i}) + \beta_{k,i} \qquad (2.13)$$

(see Figure 2.4). In this way, the calculation of the currents and the potentials in a $s \cdot z$ network is reduced to the solution of the linear equation system

/ 18

$$\left.\begin{aligned}
&R_V \cdot \sum_{i=1}^{s} I_{1,i} - \varphi^{+} = 0 \\
&I_{1,i} + \alpha_{1,i}(\varphi^{+} - \varphi_{1,i}) = \beta_{1,i} \\
&I_{k,i} - I_{k+1,i} + \frac{\varphi_{k,i} - \varphi_{k,i-1}}{R_{k,i-1}}(1-\delta_{i,1}) - \frac{\varphi_{k+1,i} - \varphi_{k,i}}{R_{k,i}}(1-\delta_{i,s}) = 0 \\
&I_{k+1,i} + \alpha_{k+1,i}(\varphi_{k,i} - \varphi_{k+1,i}(1-\delta_{k+1,z})) = \beta_{k+1,i}
\end{aligned}\right| \qquad (2.14)$$

with $i = 1, 2, \ldots, s$; $k = 1, 2, \ldots, z-1$, and the Kronecker symbol

$$\delta_{a,b} = \begin{cases} 0 & \text{for } a \neq b \\ 1 & \text{for } a = b \end{cases}$$

The first equation of system (2.14) shows the characteristic of the load resistance, while the others are the current-voltage characteristics of the converter [Equation (2.13)] and the expressions for current balance at the network junctions [Equation (2.3)].

2.3 ZUTIR Computer Program

The equation system (2.14) has the order $1 + (2z - 1)s$ and is solved by means of a digital computer. In programming, use was made of the property of the equation system that its matrix could be reduced to a band matrix of width $4s-1$ by [illegible] /19 appropriate arrangement of the equations and variables. In this way, the storage capacity of the computer is better utilized and smaller amounts of computer time are used.

As follows from Equation system (2.14), the computer program was kept as general as possible. So, for example, networks with non-uniform converters or converters with different heating can be handled, as a different characteristic can be entered for every converter. The resistances of the cross-connections can also be different.

Figure 2.5 gives a view of the working of the ZUTIR computer program.

Some results obtained with the computer program are shown in Chapter 3. These examples were based on networks in which all of the converters were identical, and could be heated constantly independent of perturbations of the network. This has the result that the transverse resistances of the network, which were likewise all assumed equal, carry no current in the case of the unperturbed network.

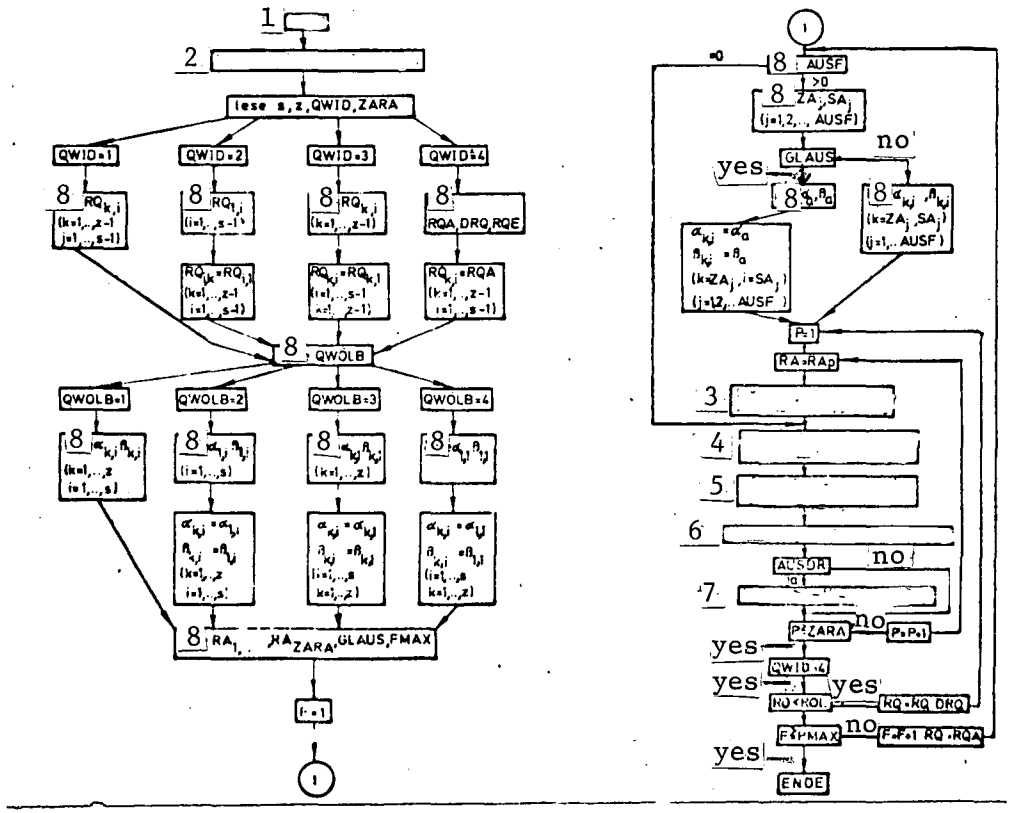

Figure 2.5: Flow diagram for the ZUTIR computer program.

1 - start; 2 - read and print clear text; 3 - print positions and parameters of the failures; 4 - set up and solve linear equation system; 5 - calculate total current, I_t, and total voltage, U_t; 6 - print RQ, RA, I_t, U_t, power; 7 - print converter I and U; 8 - read.

s : number of columns in the network

z : number of rows in the network

QWID : characteristic quantity for the treatment of transverse resistances

ZARA : number of load resistances

RQ : magnitude of one transverse resistance

RQA : first value

DRQ : step width and

RQE : final value of the transverse resistance if all are equal

QWOLB: characteristic for the treatment of characteristic curves

α : slope and

β : axial intercept of a characteristic

RA : size of a load resistance

GLAUS: characteristic magnitude of a failure

PMAX : number of different combinations of failures

AUSF : perturbed (intact) network

ZA : row of a failu e

SA : column of a failu e

AUSDR: print (do not print) working points of the individual converters

F,P,i,j,k: integral indices

3. CONVERTER FAILURES IN THE NETWORK

The lifetime of thermionic converters is studied in long-term experiments. Thus, in the Jet Propulsion Laboratory in the USA, flat radiation-heated converters were tested for their lifetime. In these studies of more than 100 converters so far (Ruklove, 1960), lifetimes of over 10,000 hours have been observed in part. Both in the USA (Howard, 1968) and in the Federal Republic (Jester, 1960), nuclear-heated converters have been operated in nuclear reactors. Various causes of failure have been established. In their final effects, they lead to two kinds of failures, idling or short circuit.

3.1 Idling

In the course of operation, the converter space or the cesium reservoir can become leaky, so that the cesium vapor escapes, and under some conditions other gases can get into the electrode gap. The internal resistance of the converter rises sharply and the current path is interrupted at this point. A break in the connecting section likewise leads to interruption of the current path. For the calculation of converter networks as described in the previous section, with idling cases, the relation between the current through the failed converter and the potential difference between its junctions must be given in a form corresponding to that of Equation (2.13). The effect of an idling converter on the currents and potentials in a network is correctly described if for the linearization constants [see Equation (2.13)] of these converters we have

$$\alpha_L \to 0 \quad \text{and} \quad \beta_L = 0$$

The physical meaning of these conditions is that a perceptible current flows through an idling converter only in the case of very great potential difference.

If a converter in the network fails due to idling, then the currents in the adjacent converters connected in series with it are likewise limited, while its neighbors connected in parallel must supply larger currents on the basis of current continuity.

TABLE 3.1: CONVERTER CURRENTS AND VOLTAGES IN A 4 x 6 NETWORK WITH AN IDLING FAILURE OF CONVERTER K(2/3)

x \ i		1	2	3	4
1	Current (A)	453,7	431,9	365,9	421,6
	Voltage (V)	0,607	0,660	0,820	0,685
2	Current (A)	519,1	564,9	0,0	589,1
	Voltage (V)	0,447	0,336	0,008	0,277
3	Current (A)	447,1	430,2	371,9	424,0
	Voltage (V)	0,623	0,664	0,806	0,679
4	Current (A)	425,6	420,2	412,0	415,3
	Voltage (V)	0,675	0,683	0,708	0,700
5	Current (A)	420,2	418,8	417,1	416,9
	Voltage (V)	0,688	0,691	0,696	0,696
6	Current (A)	418,9	418,5	418,0	418,0
	Voltage (V)	0,691	0,692	0,694	0,694

Table 3.1 gives the converter currents and the potential differences between their junctions (the converter voltages) in a network with an idling failure of converter K(2/3). The load resistance was selected so that all converters of the undisturbed network operate at a current of 435 amperes and a voltage of 0.65 volts. Under these conditions, the

/ 23

remaining converters develop only a small potential difference between the junctions of the failed converter, as the equality of the potentials of all converter gaps is ensured by the fact that the gaps of the failed converters operate at higher potential than the others.

According to Equation (2.8) the cooling of the emitter is proportional to the converter current. Therefore, a change in the current causes a change of the emitter temperature, as long as the emitter heating remains constant. In particular, the emitter temperature increases sharply if the electron cooling is interrupted due to an idling failure. Table 3.2 shows the emitter temperatures of the converters of the network for which the currents and voltages were given in Table 3.1. The emitter temperatures in the undisturbed network were 2,000°K. The emitter temperatures were determined from the working points of the converters (Table 3.1) with the help of the heat balance (see Section 2.1.2).

TABLE 3.2: EMITTER TEMPERATURES (IN °K) OF THE CONVERTERS OF A 4 x 6 NETWORK WITH AN IDLING FAILURE OF THE CONVERTER K(2/3)

k \ i	1	2	3	4
1	1978	2004	2094	2016
2	1900	1830	>2500	1808
3	1986	2002	2084	2012
4	2011	2018	2026	2023
5	2018	2020	2022	2022
6	2020	2020	2071	2021

3.2 Short Circuit

At the high temperatures of the emitters ($T_E \approx 2000°K$), the emitter materials can vaporize to a small extent, precipitate on the cooler collector, and in this way form conducting bridges between the emitter and the collector. Thus, the voltage across this converter breaks down. Also, conducting foreign bodies which get into the electrode gap due to material failures, as well as from the swelling of the fuel in nuclear heated converters, can cause a short circuit. The current density flowing through the electrode gap of a short-circuited converter in a network can be determined by use of Figure 2.4. The increased current density is not perceptible in the network, however, as the converter current flows back over the short circuit bridge. Thus, a short-circuited converter behaves in the network like a resistance consisting of the ohmic resistance of the electrodes and the connecting section. The linearization constants of the converter then transform on short circuit into

$$\alpha_K = \frac{1}{R_{EC}+R_{vs}} \quad \text{or} \quad \beta_K = 0$$

The direction of net current flow across a short-circuited converter depends on the potentials developed by the other converters at its junctions. Table 3.3 gives the distribution of the currents and voltages in the network described in the previous section, where converter K(2/3) is assumed to have been destroyed by a short circuit. Because of the short circuit, the converters of the same row of the network cannot form any large voltages. In contrast, the voltage of the adjacent converters of the same column increases because, as in the case of idling, their currents must be conducted past the failed converter.

The emitter temperature drops when a converter is short-circuited because of the increased electron cooling, as can be seen from Figure 2.4.

/ 25

TABLE 3.3: CONVERTER CURRENTS AND VOLTAGES IN A 4 x 6 NETWORK WITH A SHORT CIRCUIT FAILURE OF THE CONVERTER K(2/3)

k \ i		1	2	3	4
1	Current (A)	453,9	431,9	365,1	421,4
	Voltage (V)	0,606	0,660	0,822	0,685
2	Current (A)	520,1	566,4	-5,0	590,8
	Voltage (V)	0,445	0,332	0,0	0,273
3	Current (A)	447,2	430,1	371,1	423,8
	Voltage (V)	0,662	0,664	0,807	0,679
4	Current (A)	425,4	420,0	411,7	415,1
	Voltage (V)	0,675	0,689	0,709	0,700
5	Current (A)	420,0	418,6	416,9	416,7
	Voltage (V)	0,689	0,692	0,696	0,697
6	Current (A)	418,7	418,3	417,8	417,5
	Voltage (V)	0,692	0,693	0,694	0,695

3.3 Significance of the Transverse Resistances

On comparison of Tables 3.1 and 3.3, short circuit and idling appear to correspond to the shift of the working point and thus to the emitter temperatures of the other converters. But this is in no way always the case, because the effect of the failure depends strongly on the electrical resistance of the transverse connections. With low resistances, the coupling between the individual columns of the network is relatively strong, so that no large differences can appear in the voltages of the converters of a row. As a result, the differences in the currents and, therefore, of the emitter temperatures of the converters adjacent to a failed one are / 26 diminished. This desirable property is not provided for large transverse resistances. Here, then, the emitter temperatures of the adjacent converters connected in series with the failed one increase strongly, especially with an idling failure (Figure 3.1). These increased emitter temperatures could cause a failure of the converter concerned, so that a chain of failures could be set off. In spite of this serious behavior, it is

not advantageous in every case to use low transverse resistances. The fact that the power loss of a converter due to converter failure also depends on the magnitude of this resistance (Figure 3.2) argues against it. With short circuits, the power loss is smaller, the greater the transverse resistances are. With idling, the conditions are exactly the opposite. The rule of thumb given in the literature (Homeyer, 1968), that the power loss of a network in percent is about twice as great as the percentage of failed converters, is confirmed by Figure 3.2.

In designing the transverse resistances of a network, one should consider not only their effect on the increase of emitter temperatures, but also on the loss of power, according to the possibility of their technological realization. A resistance of the magnitude of 10^{-3} to 10^{-4} ohms appears to be consistent with these viewpoints.

/ 27

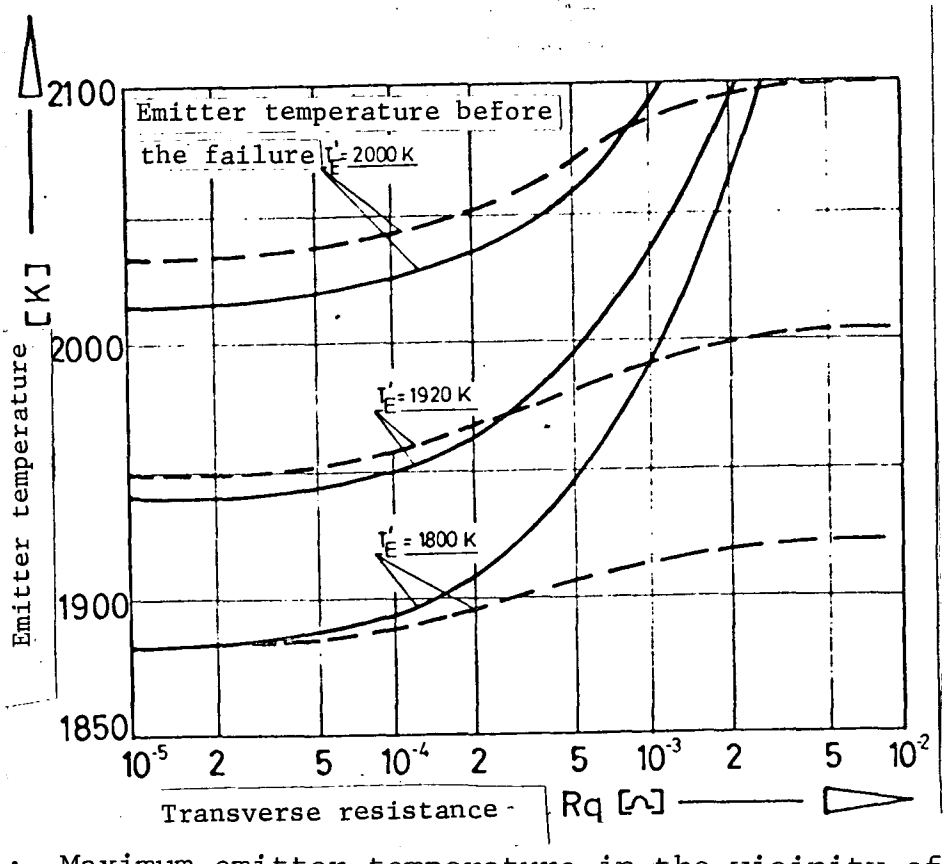

Figure 3.1: Maximum emitter temperature in the vicinity of a converter failed due to idling (——) or short circuit (- - -).

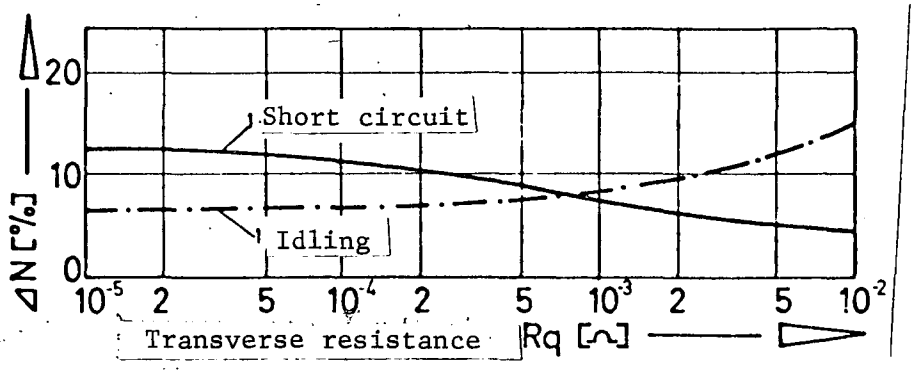

Figure 3.2: Power loss of a 4 x 6 converter network due to a failure.

/ 28

3.4 Statistical Treatment of Converter Failures

The reasons for failure of thermionic converters were stated in the previous section. In order to learn more in detail about these reasons, numerous experiments have already been performed. Conclusions on the possible improvements of converters have been obtained from them. The lifetimes of converters with different operating conditions have also been tested in such long-term tests. Thus, for example, Rouklove (1968) states that the lifetime of his converters decreased by a factor of about two if he increased the emitter temperature by 50°K. The General Electric Company (USA) operated converters in a reactor for over 3,600 hours before a short circuit occurred (Hoomissen, 1968). Certainly great advances in converter technology will be attained before the employment of thermionic reactors for spacecraft power supply. In spite of that we can assume that in the forseeable future the probability of failure of converters will not be considered negligibly small for the design of such systems. Also, neither the time of a failure nor its position in the network will be known in advance. It can only be predicted with statistical probability. Therefore we can only obtain a prediction of the operating reliability of converter networks on the basis of the statistical method. The solution of this

problem is the object of this investigation. The methods used will be outlined in the following sections.

3.4.1. Number of failures during operation

The probability of a particular converter failing in the course of a giving operating time depends on many parameters, and particularly on the emitter temperature. It can be determined only with long-term tests on many converters of the same type. This probability is made up of two parts: the probability p_K of a short circuit within a specified operating time, and the probability p_L that a converter will fail through idling. These failure probabilities are treated as parameters in the following investigations. / 29

The probability that, out of N converters in a system, A will fail, when P is the probability for a single failure, is given by Newton's formula

$$P_{N,A} = \binom{N}{A} p^A (1-p)^{N-A} \qquad (3.1)$$

Now if two different types of failure occur, then in place of Equation (3.1) we have

$$P_{N,K,L} = \binom{K+L}{N}\binom{K}{K+L}(p_K)^K(p_L)^L(1-p_K-p_L)^{N-K-L} \qquad (3.2)$$

with the designations: K = number of short-circuited converters; L = number of idling converter failures. This equation indicates the magnitude of the probability that, in a network with N converters, for which the failure probabilities are p_K and p_L, K converters will fail by short circuit and L through idling. These probabilities are shown in Figure 3.3.

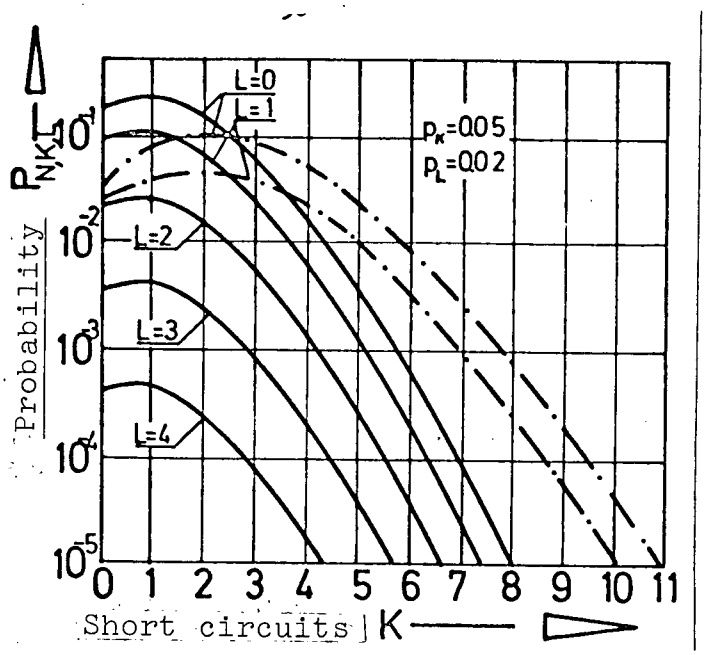

Figure 3.3: Probability of the occurrence of K short circuits and L idling converters in a network with 24 (——) or 48 (- · - ·) converters, for assumed values of p_K and p_L.

3.4.2. Effect of the positions of the failed converters on the power of a network.

The effect of converter failures on the characteristic data of a network (power, emitter temperature, etc.) depends on their position in the network. This is clarified in Table 3.4. Power losses in comparison to the undisturbed network were calculated for ten different positions (determined by random numbers) of four short-circuited and three idling converters in a 6 x 8 converter network. The loss varies between 25% and 31.1% (see Table 3.4).

TABLE 3.4: EFFECT OF FAILURE POSITIONS ON THE POWER LOSS OF A 6 x 8 NETWORK

Failed converters K(k/i)		Power loss
By short circuit	By idling	(%)
K(6/3) K(6/1) K(5/5) K(7/4)	K(3/3) K(1/4) K(6/5)	25,5
K(8/6) K(8/1) K(6/3) K(1/6)	K(5/3) K(3/4) K(1/3)	25,1
K(1/3) K(4/5) K(5/4) K(3/4)	K(6/1) K(8/1) K(4/6)	31,1
K(6/3) K(5/1) K(6/4) K(1/6)	K(7/3) K(2/3) K(5/2)	25,0
K(5/4) K(6/3) K(4/3) K(1/6)	K(4/5) K(5/3) K(6/2)	28,4
K(7/4) K(5/6) K(6/3) K(3/6)	K(6/6) K(5/1) K(8/4)	29,4
K(6/2) K(8/2) K(1/2) K(4/5)	K(1/3) K(3/3) K(5/5)	26,4
K(8/1) K(3/5) K(5/3) K(4/5)	K(1/6) K(6/4) K(2/5)	27,2
K(1/5) K(6/2) K(7/2) K(1/2)	K(5/4) K(3/4) K(1/6)	28,4
K(8/3) K(4/3) K(6/5) K(4/5)	K(3/4) K(4/6) K(4/4)	28,2

On the assumption that all converters have the same failure probability (independent of their position in the network and the operating conditions), we can determine the probability that the power will drop by a certain value ΔN in case of K + L converter failures. In order to solve this problem exactly, the power loss must be calculated for every possible permutation of failure combinations. For a network with N converters and one failure, N/4 network calculations are necessary, for reasons of symmetry. For two indistinguishable failures, (N)N - 1)/2)/4 calculations are needed. For the general case of A failures in a network of N converters,

$$\frac{N!}{4(N - A)!A!}$$

calculations are necessary. If two different types of failures (idling and short circuit) can exist together, then the number of calculations needed to determine the distribution of

power losses for a certain number, $K + L$, of converter failures is

$$\binom{N}{K+L}\binom{K+L}{L} / 4$$

It is easily perceived that this exact solution of the problem which has been set up requires excessive computing cost even for small networks. The cost can be reduced significantly by means of statistical methods, with which, for each number $K + L$ of failed converters, one determines their positions in the network several times by random numbers, calculating for each case the power loss ΔN_i ($i = 1, 2, \ldots, i_{max}$). From such random sampling of the extent i_{max} (i_{max} is 50 to 100), we can draw conclusions on the most probable distribution of power losses for $K + L$ failures (see Lindner, 1964). /32

Figure 3.4 shows the result of a sampling test of the power losses of a 6 x 8 network due to the failure of four converters in short circuit and three due to idling, in the form of a frequency distribution.

3.4.3. Calculation of the probability for the occurrence of a certain power loss.

With constant heat input to the converter and constant load resistance, the power loss increases, in general, with the number of failed converters. It is easily understood, however, that, for instance, four idling failures in one row of a network can cause a greater power loss than five such failures distributed evenly across the entire network. This fact, that $A + i$ failures could cause less power loss than A failures, leads to overlapping of adjacent frequency distributions $h_A(\Delta N)$ and $h_{A+i}(\Delta N)$. In determining the probability that the power loss due to converter failures will take on a certain value $\Delta N'$, therefore, it is generally necessary to consider that this power loss can occur with not

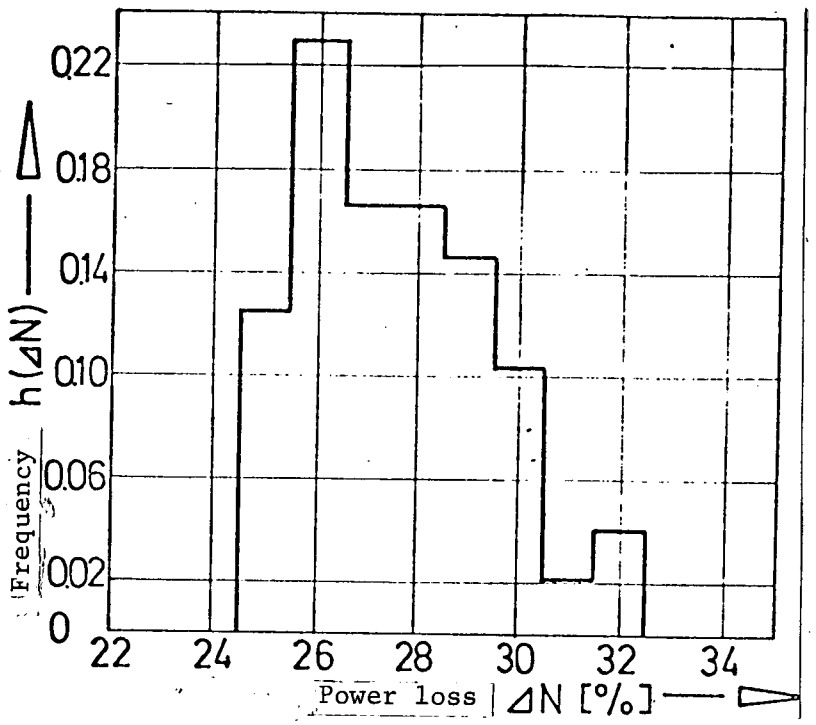

Figure 3.4: Frequency of appearance of the power loss ΔN in 60 calculations for four short circuits and three idling failures in a 6 x 8 network.

just a single number of failures. Rather, the probability of power loss by a certain amount $\Delta N'$ is in general equal to the sum of the individual probabilities for the failures which lead directly to this power loss, multiplied by the matching probabilities that the number of failures under consideration will lead to this power loss:

$$w(\Delta N') = \sum_{A=1}^{N} P_{N,A} h_A(\Delta N') \qquad (3.3)$$

Calculation of the probability $P_{N,A}$ was described in Section 3.4.1. For the probability $h_A(\Delta N')$, the values from the corresponding frequency distributions (see Figure 3.4) could be inserted. For practical calculations, however, this

route is very tedious. For that reason, an approximation of the frequency distribution by analytical functions was undertaken. / 34

An analytical representation of the frequency distribution has the advantage that the desired value $h_A(\Delta N')$ can be calculated from a few parameters which are characteristic for the corresponding distribution. Many such problems occur in mathematical statistics (Lindner, 1964).

In statistical methods, the most frequently occurring distribution of one property in the total set is the biparametric normal distribution

$$f(x)dx = \frac{1}{\sqrt{2\pi}\sigma} \exp\left(\frac{(x-\mu)^2}{2\sigma^2}\right)dx \qquad (3.4)$$

with the parameters μ and σ, which are calculated from empirical values of X_i by

$$\mu = \frac{1}{I_{max}} \sum_i x_i \qquad (3.5)$$

and

$$\sigma^2 = \frac{1}{I_{max}-1} \sum_i (x_i-\mu)^2 \qquad (3.6)$$

This distribution is symmetrical about the mean μ. But the frequency distributions $h_A(\Delta N)$ show a distinct asymmetry (see Figure 3.4). This can be explained qualitatively by the fact that the random distribution of failures in the network produces relatively small power losses, while large power losses due to short circuits of several converters connected in series or idling of several connected in parallel occur with lower probability.

By means of the coordinate transformation / 35

$$x = (\Delta N - C) \qquad (3.7)$$

the frequency distributions $h_A(\Delta|N)$ are transformed into approximately symmetrical distributions $h_A(x)$, which can be approximated well by biparametric normal distributions. The parameters of these distributions are determined through Equations (3.5) or (3.6) with

$$x_{A,i} = (\Delta N_{A,i} - C_A). \tag{3.8}$$

By variation of the third parameter C_A of the distributions, at first taken to be arbitrary, we can achieve the condition that the empirical $h_A(x)$ and the matching analytical distribution $\bar{h}(x)$ differ as little as possible:

$$\int_{x=0}^{\infty}(h_A(x)-\bar{h}_A(x))^2dx = \text{Min} \tag{3.9}$$

The analytical distribution $h_A(\Delta|N)$ for matching to the empirical frequency distribution $h_A(\Delta|N)$ then arises from Equation (3.4) after insertion of Equation (3.7) with the optimum matching constant C'

$$\bar{h}(\Delta N)d(\Delta N) = \frac{1}{\sqrt{2\pi}\,\sigma(\Delta N-C')}\exp\left(\frac{(\ln(\Delta N-C')-\mu)^2}{2\sigma^2}\right)d(\Delta N) \tag{3.10}$$

Examples of this matching are shown in Figure 3.5 with A = 2, 5, 10, and 15 (short circuit failures) in a 6 x 8 converter network.

If we insert the expressions of Equations (3.2) and (3.10) for $P_{N,A}$ and $h_A(\Delta|N')$ into Equation (3.3), then we get the following expression for the probability of occurrence of the power loss $\Delta|N'$ in a network with N converters

/ 37

$$w(\Delta N') = \sum_{A=0}^{N}\sum_{L=0}^{A}\binom{A}{N}\binom{L}{A}(p_K)^K(p_L)^L(1-p_K-p_L)^{N-A}\cdot \cdot\frac{\exp\left(\frac{(\ln(\Delta N'-C'_{K,L})-\mu_{K,L})^2}{2\sigma^2_{K,L}}\right)}{\sqrt{2\pi}\,\sigma_{K,L}(\Delta N'-C'_{K,L})} \tag{3.11}$$

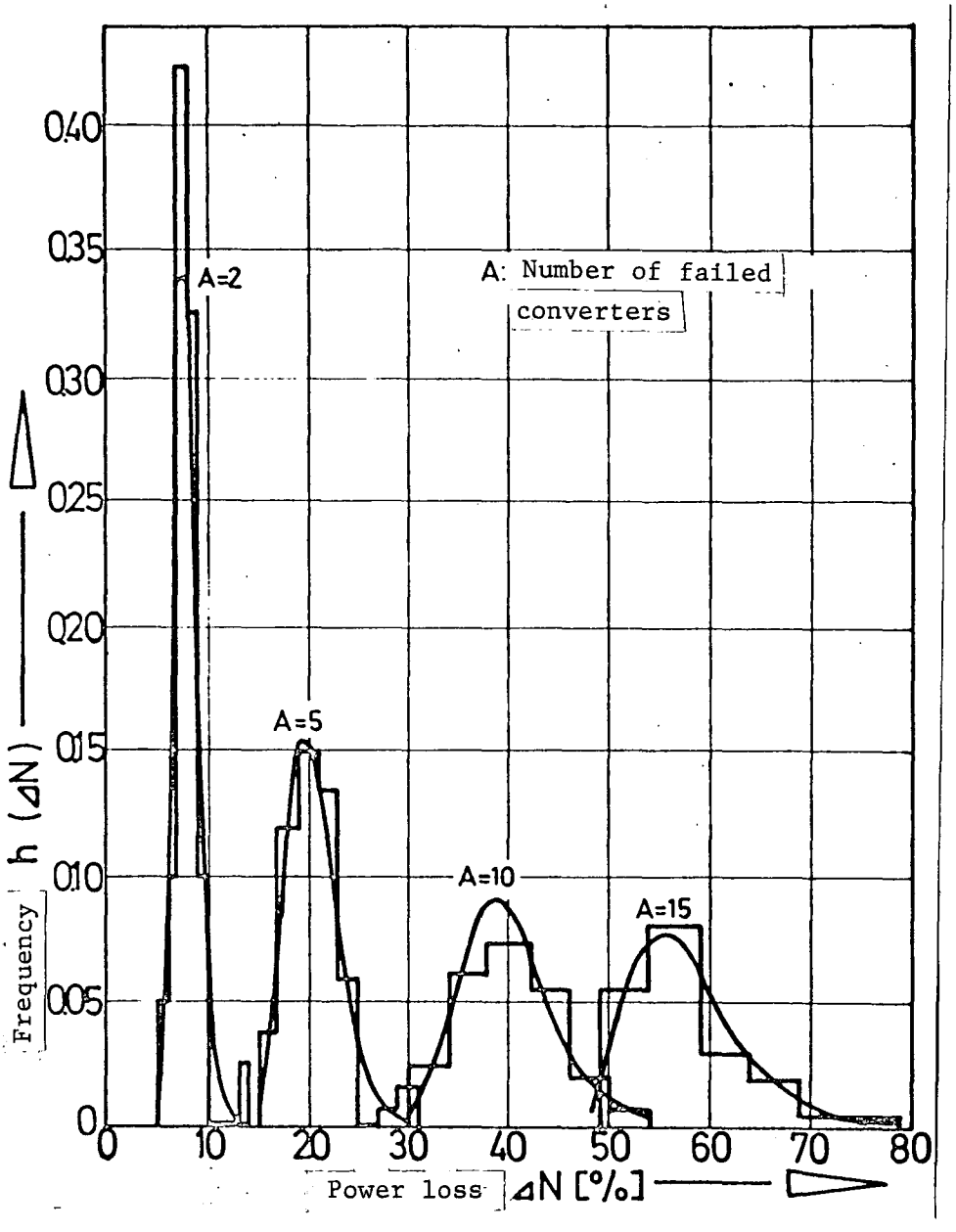

Figure 3.5: Empirical and matched analytical frequency distributions.

3.4.4. Reliability diagram

To judge a power supply system, knowledge of its reliability is of great importance. Thus, the reliability, Z, is defined as the probability that the required nominal power can be produced. For the thermionic power supply systems treated here, the reliability can be determined by means of Equation (3.11), under the applicable assumptions (see Section 2.3). Understandably, this depends on how great a portion of the potential initial power is supplied as the nominal power ΔN_N. Expressed as the power loss ΔN, the reliability is given by the probability that $\Delta N \leq 1-\Delta N_N$.

$$Z(\Delta N) = \int_0^{1-\Delta N_N} w(\Delta N')\, d(\Delta N') \qquad (3.12)$$

Figure 3.6 shows this reliability for a 6 x 8 network, calculated after use of Equations (3.11) and (3.12).

For investigations which serve only the purpose of determining significant predictions about the behavior of converter networks in case of failures, it is in general sufficient to use less demanding approximations in place of the strict relation (3.12).

In particular, the high cost of computation can be reduced by ascribing a power loss $\Delta N(A)$ to a certain number of converter failures. As an example, we can use for this the mean power loss from some few combinations of failure positions. Even the use of the results of a single network calculation for each number of failures can in many cases be considered sufficiently accurate to determine the reliability diagram for a network. The points plotted in Figure 3.6 were determined in this way. / 39

The graphic presentation of the reliability as a function of the power loss is called the reliability diagram for the network concerned. This dependence is shown for two different

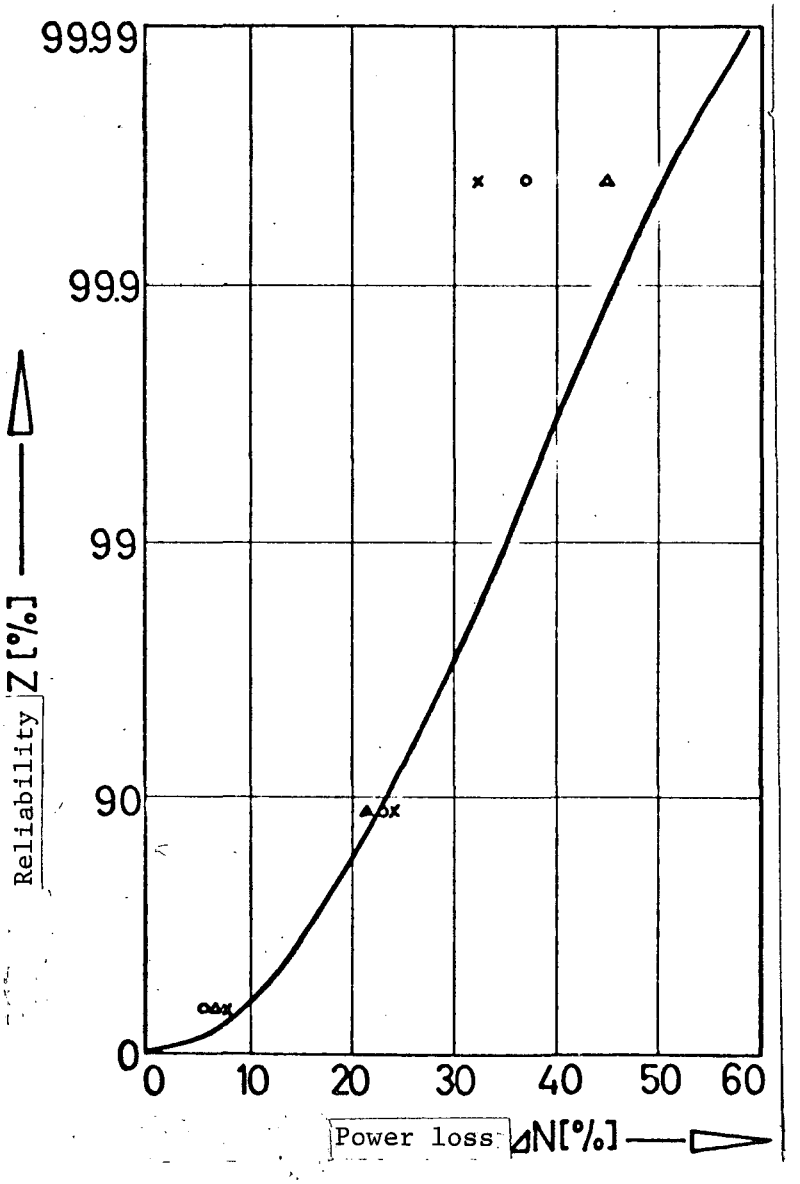

Figure 3.6: Reliability of a 6 x 8 network calculated according to Equation (3.12) and a less expensive approximation.

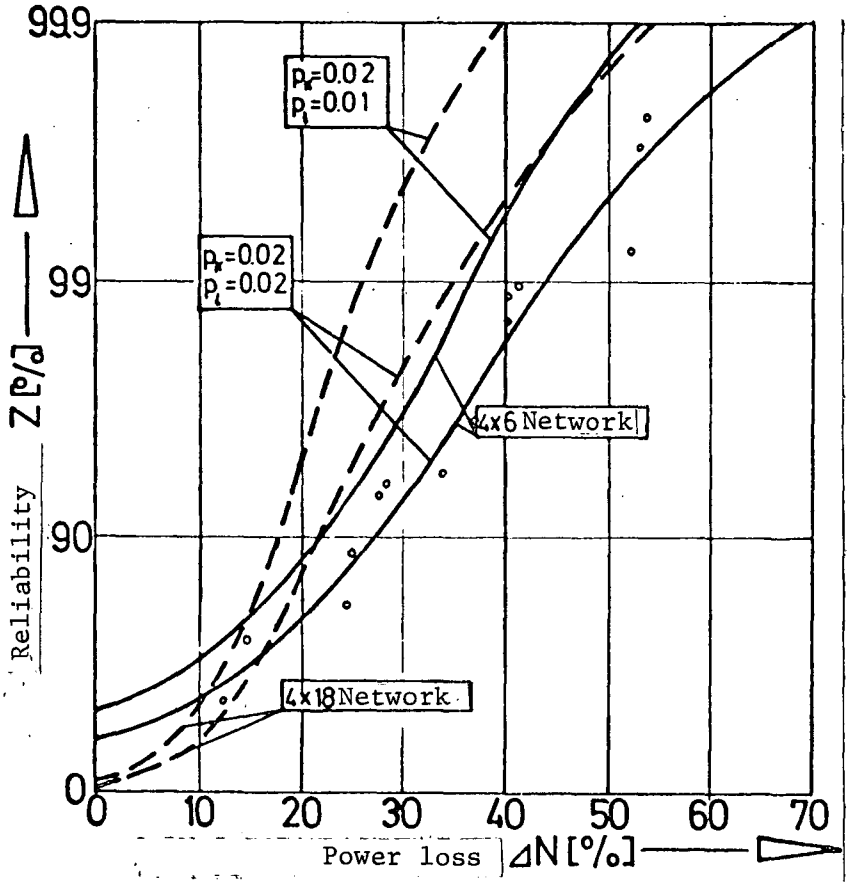

Figure 3.7: Reliability diagrams for two networks with short circuit and idling failures.

networks in Figure 3.7. Some interesting conclusions can be drawn from this figure. Thus the reliability of a network, even explained indirectly, is higher the more reliable the individual converters are. Here the reliability of a network is defined as the probability that a prescribed power loss will not be exceeded.

This figure also shows that in the range of interest ($Z \geq$ ca. 90%), large networks are more reliable than small ones.

/ 41

4. EFFECT OF CONVERTER FAILURES ON THE OPERATION OF THE PARTIALLY THERMIONIC REACTOR ITR

In order to guarantee satisfactory operation of a consumer of current, it must be supplied with its rated power at a specified voltage. Therefore it seems reasonable to require that a thermionic power supply system will provide a given rated power at constant voltage over a specified operating time. Because of this condition, systems with constant heat input [heating of the converter by long-lived radioisotopes (Gammel, 1968) or solar radiation (Merra, 1963)] can in general be designed only for part of the power which could be produced by the undisturbed network (see Section 3.4.4). At the beginning of the operating period of such systems, then, it is necessary to destroy the excess power (e. g., in electrical resistances) or to operate the converter at low efficiency, although this means a change in the terminal voltage.

When a nuclear reactor is used as a heat source for a thermionic converter network, the heat input can be adjusted to the power and voltage required at the time. As long as all the converters are still intact, the reactor can be operated at a lower thermal power than necessary at a later time to maintain the electrical rated power. In comparison to operation at constant thermal power, this mode of operating

has the advantage that the converter is less stressed (lower emitter temperatures and power density). Also, the consumption of the nuclear fuel is diminished. In this way, part of the mass required for the initial excess reactivity of a space reactor can be saved.

In the remaining sections, we show by means of an example a method by means of which we can predict the probability of change in some operating parameters of a thermionic reactor converter due to converter failures. / 42

4.1 Description of the Reactor

4.1.1. Reactor design

The fission zone of the partially thermionic reactor consists of the central thermionic zone, which is surrounded by the driver zone which is necessary for reasons of criticality (Figure 4.1). In the design on which this is based, 19 fuel rods are planned in the thermionic zone. Each of these consists of seven thermionic converters connected in series, a cooling channel, and a moderator prism. The nuclear fuel (ca. 50 g of UO_2) is placed in holes in the molybdenum emitter bodies (Budnick, 1968).

4.1.2. Power distribution

In a converter cell heated by fission of the fuel nuclei enclosed within the emitter, the thermal power is

$$\Omega_z = \int_{V_z} \int_E \phi(\mu, E)\Sigma_f(\mu, E)\,dE\,dV \qquad (4.1)$$

Because of the neutron leakage loss from the reactor surface, the neutron flux density $\phi(\mu, E)$ and, therefore, the thermal cell power within the reactor fission zone are in general dependent on position. Wolf (1968) has shown that uneven heating of identical converters along a fuel rod results in a severe drop

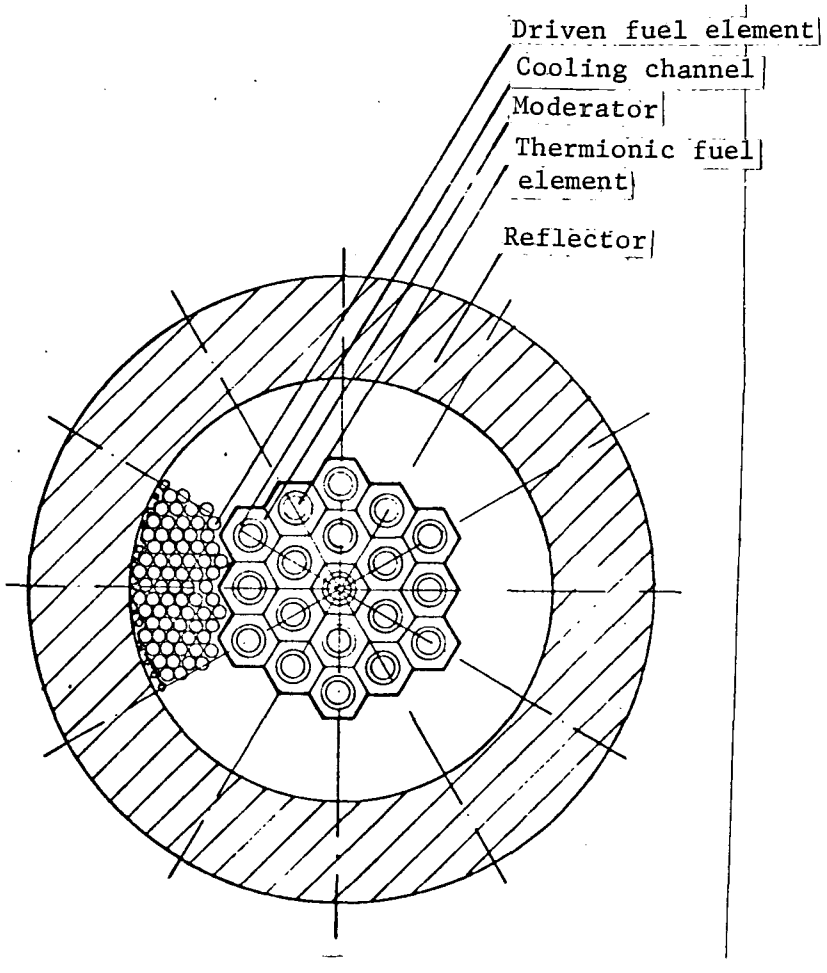

Figure 4.1: Cross section of the partially thermionic reactor (ITR).

in converter efficiency and, therefore, in the electrical power. / 44
By appropriate connection of the fuel rods in a series-parallel network the undesired effect of uneven heating of the individual rods can be diminished, although not eliminated.

In the case of the ITR, these disadvantages are eliminated by the leveling of the power density in the thermionic zone. This is achieved in the axial direction by a change in the N_H/N_{U-235} ratio, while we can undertake the leveling in the radial direction by appropriate design of the driver zone. For this concept, then, it can be assumed that all the converters exhibit the same characteristics.

4.1.3. Converter characteristics

Brown, Boveri & Co. have built appropriate converters for use in the partially thermionic reactor ITR, and tested them both in the laboratory and in the neutron flux from nuclear reactors. The characteristics shown in Figure 4.2 were recorded in such test operations. The dashed characteristic lines in this diagram were measured at constant power for the test reactor used. They are not suitable as bases for reliability studies, however, as the power liberated in the emitter was not stated. The present study is based on characteristics determined by means of a computer program (Haug, 1968) at a cesium pressure of about 6.6 Torr (Figure 2.4). With this program, the two-dimensional temperature distribution in the emitter body is calculated, with the theoretical converter model of Rasor (see Section 2.1.1) used as the boundary condition at the emitter surface. Due to the dissimilar boundary conditions at the ends of the emitter body (greater heat removal through the connecting section at one end) there appears an uneven temperature distribution / 46
and current density distribution along the emitter surface. We obtain the desired relation between the converter current and its voltage by multiplying the current density shown in

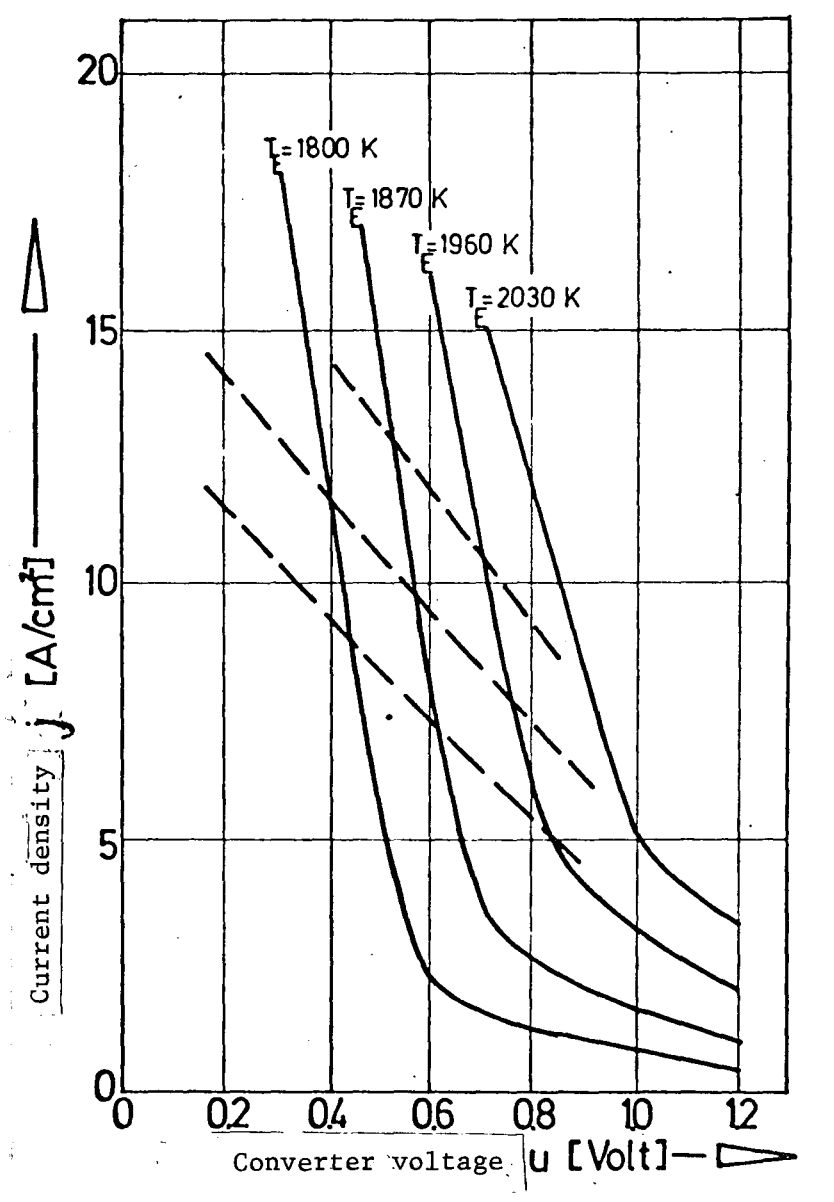

Figure 4.2: Current-voltage characteristics for a nuclear-heated converter (- - - constant heat input).

Figure 2.4 by the emitter surface area of 34 cm^2, as the data for this figure represent averages for the converters.

For an exact calculation of the reliability behavior of a converter network it is necessary to base it on the experimentally determined characteristics of the converter in question. However, it is the object of this study to show the method for such studies, so the use of calculated characteristics is justified.

4.2 Converter Network Connections

4.2.1 Reliability of the converter system without cross connections

Previous publications about the ITR partially thermionic reactor have contained no information on the network connections of the converters. The design allows parallel connection only between the converters at the ends of the fuel rods. In case of an idling failure, then, all the converters of the same fuel rod fail in sympathy, as they likewise can draw no current.

This great power loss in case of an idling failure requires large excess capacity for the intact network ($N_{excess} = N_{intact} - N_{rated}$) in order that the rated value can be produced with acceptable reliability ($\geq$ 90%). Even the assumption of 98% reliability of a converter with respect to idling requires an excess capacity of around 100% for 99% probability of maintaining the rated power (solid curve in Figure 4.3).

By connecting the converters of the reactor in a network / 47
it is theoretically possible to make a considerable increase of reliability in the range of interest, with the same excess capacity (dashed curve, Figure 4.3).

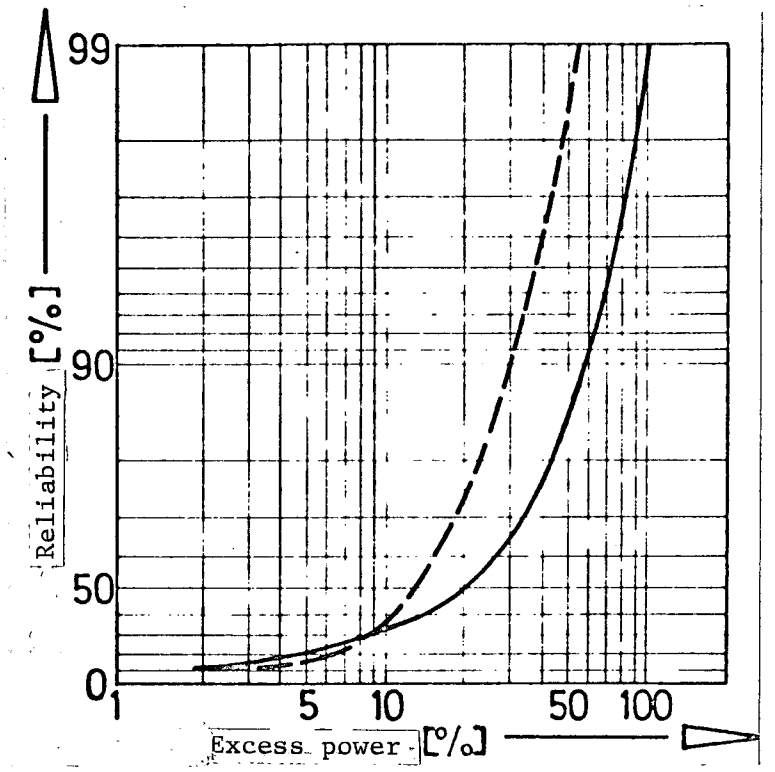

Figure 4.3: Excess capacity needed to maintain the rated power of an ITR converter system with (- - -) and without (——) cross connections.

4.2.2. Design of cross connections / 48

Conversion of the theoretical results into practice requires study of the design possibilities by which cross connections could be made between the individual converters of a thermal incore thermionic reactor. The solution of this problem provides an extension of the present three-layer tube by an insulating and a conducting layer (Figure 4.4). Over the individual, mutually insulated segments of the conductor tube produced in this manner, which are connected to the separate collectors of the fuel elements (Figure 4.5), the current can be conducted to the ends of the fuel elements in case of a converter failure.

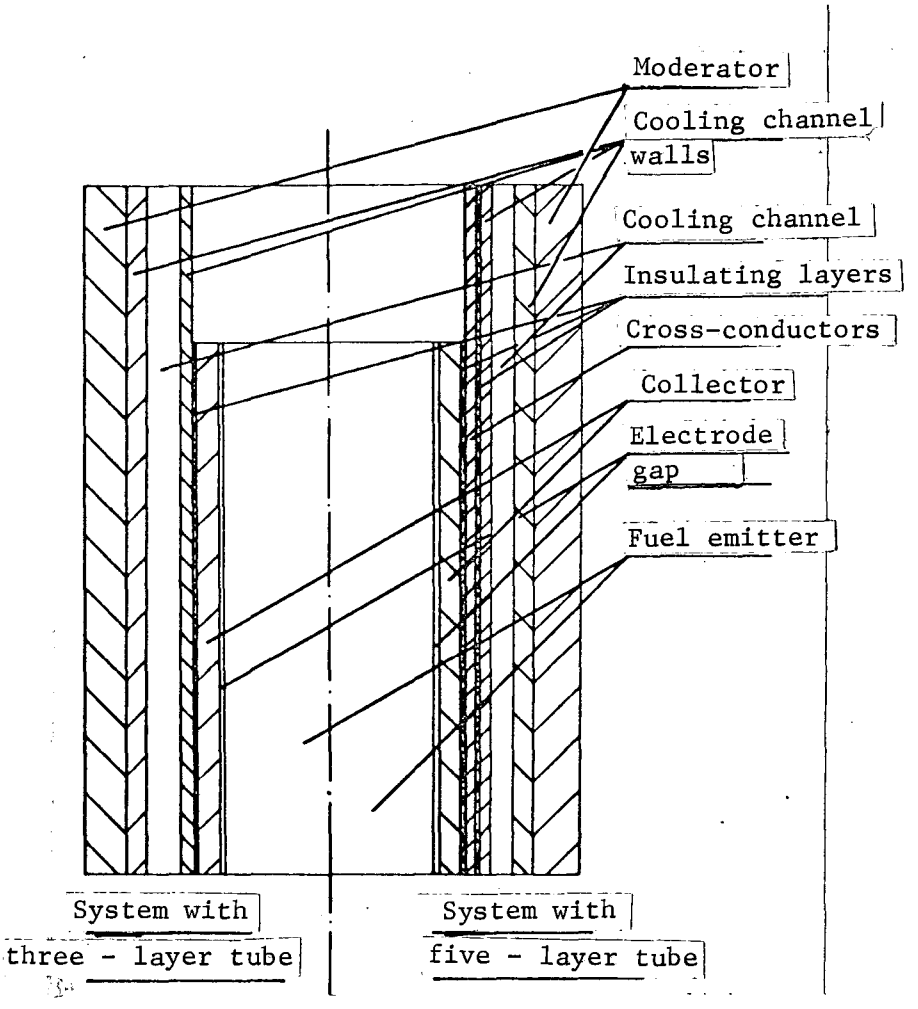

Figure 4.4: ITR thermionic cell with three-layer tube (left) and five-layer tube (right).

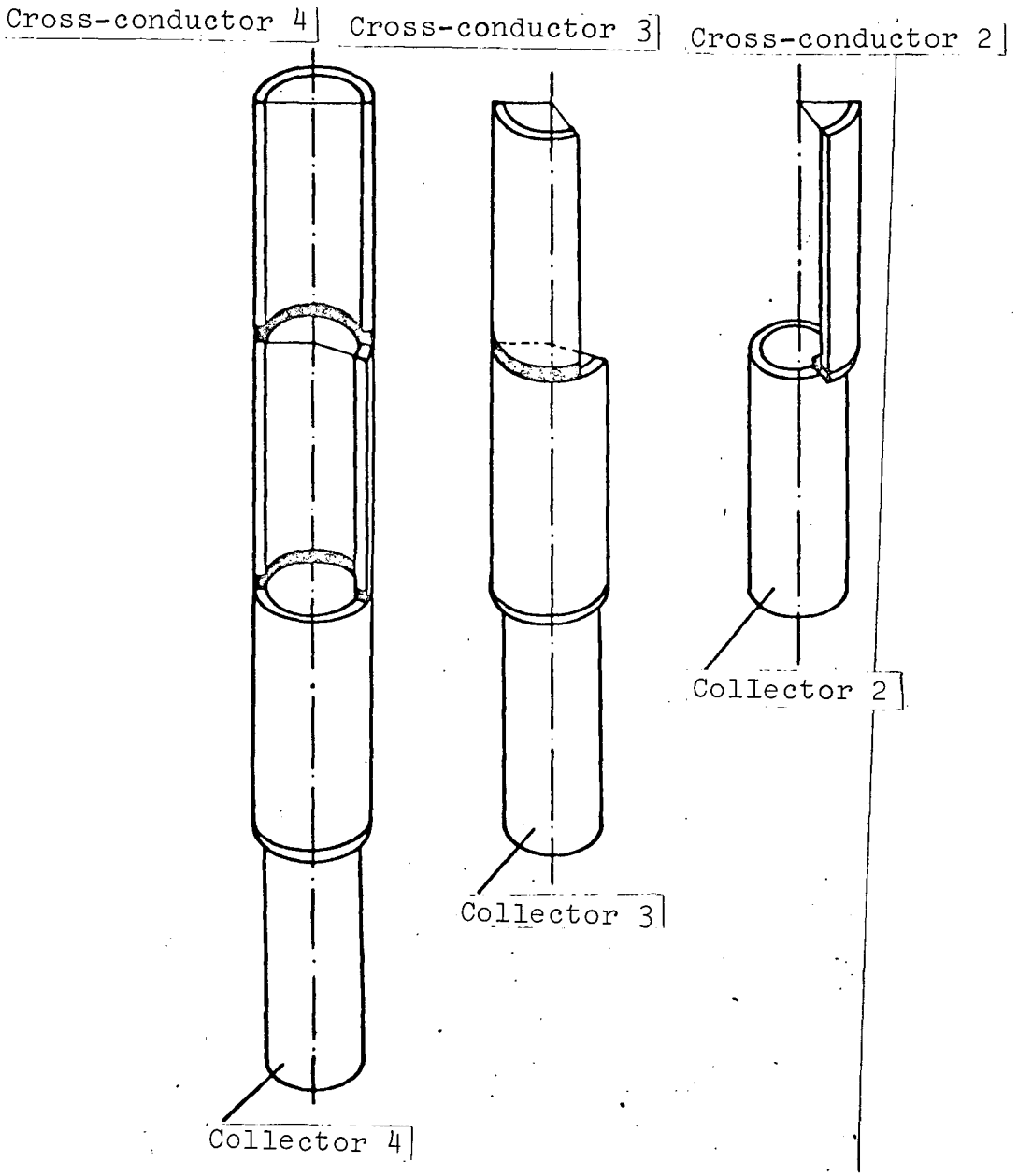

Figure 4.5: Extension of the collector system of an ITR fuel rod to allow parallel connections between the individual converters.

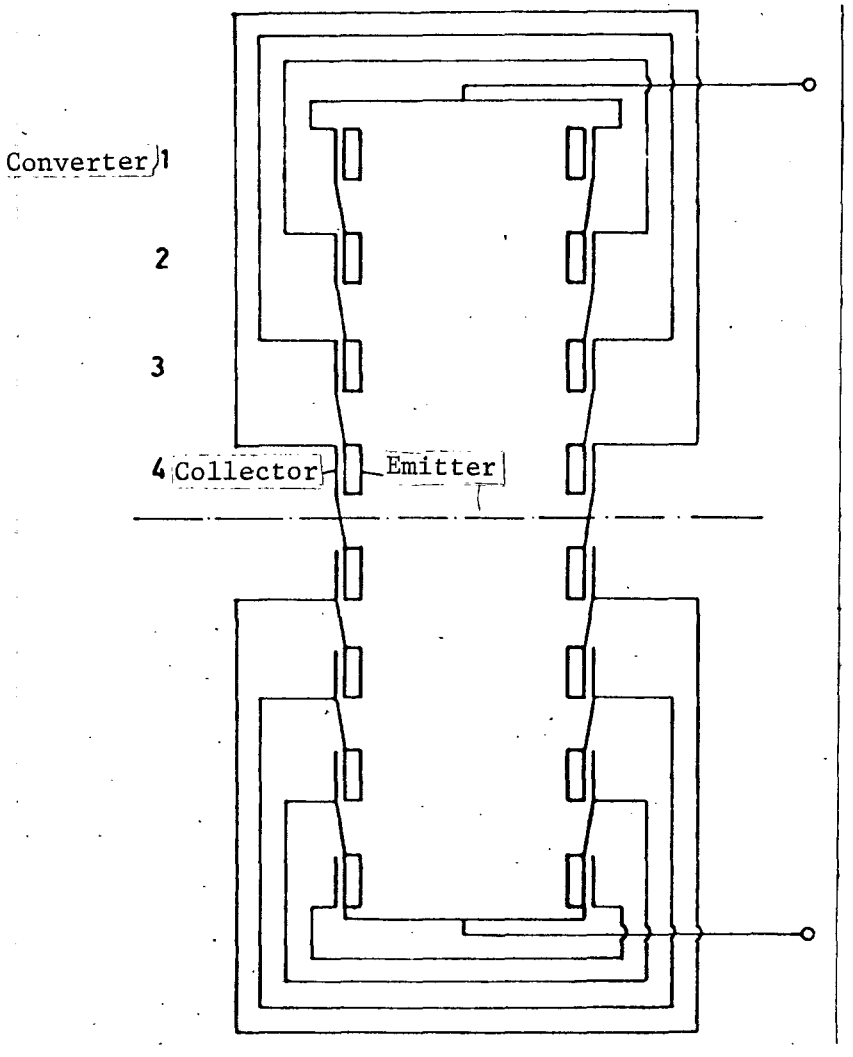

Figure 4.6: Principle of the parallel connection of the converters of two fuel rods.

There an arbitrary parallel connection of the converters can be undertaken. Figure 4.6 shows the parallel connection of the corresponding converters of two fuel elements with eight converters each.

In order to obtain an electrical resistance of a reasonable order of magnitude (see Section 3.3), the wall thickness of the conductor tube must be from 1 to 3 mm. This increases the separation between the fuel and the moderator, by insertion of neutron-absorbing materials. This has an undesirable effect on the neutron balance of the cell. In the case of the ITR, this disadvantage is only of secondary importance because of the great reactivity reserve of the driver zone.

4.2.3 Resistance of the cross connections

On idling failure of a converter of the ITR thermionic fuel element, the emitter temperature of the converter involved increases sharply (see Section 3.1). The temperatures which occur in this way increase the creep rate and the vaporization rate of the emitter material (molybdenum) to a great extent. This justifies the assumption that conducting /52
bridges will form between the emitter and the collector. In this way idling, if it is not caused by breakage of a connector, changes into an electrical short circuit. For the design of the parallel connections of this thermionic reactor concept, this assumption has the consequence that their resistances can no longer be chosen solely according to the viewpoints mentioned in Section 3.3. Rather, we need only consider that the temperatures occurring in the neighborhood of an idling converter during the time in which the idling transforms into a short circuit must not destroy them or leave permanent damage. The calculations in Section 4.3 were based on transverse connections with an electrical resistance of 10^{-3} ohms.

4.2.4 Cesium supply

An idling failure is generally caused by a leak in the cesium vapor space or in the reservoir of the converter in question, as a break in the connecting piece can be considered highly improbable. The advantage of parallel connections between the converters does not come to bear, then, as long as several converters (e. g., all the converters of one fuel rod) are supplied from the same reservoir. Each converter can be supplied with cesium vapor independently by installing a reservoir in the form of a sintered metal or graphite body in the converter space (Yates, 1968). Such reservoirs, in which the cesium is stored either at the surfaces (external and internal) of a porous sintered metal matrix or in the form of a chemical compound (C_xCs) maintain a cesium pressure in the converter space which depends generally on the emitter and collector temperature of the converter concerned, and which can be adjusted by the amount of cesium charge. Otherwise, no control of the cesium pressure is possible.

4.2.5 Network geometry / 53

In connecting the converters into a network, we must strive for an arrangement which allows all the converters to work at the same operating point. This condition is met for an ITR network only if both the rows and the columns contain equal numbers of converters.

But such an arrangement is possible with the 19 x 7 converters of this design only if all the fuel rods are connected in parallel.

For the present study, therefore, the central rod was not considered. In consideration of the viewpoints mentioned in Section 3, a network was designed which contained three rods in series and six in parallel (6 x 21 network).

4.3 Calculation of the power level and the emitter temperatures at the end of a prescribed operating time

4.3.1. Assumptions for the calculation

The reliability of a converter network depends particularly on the failure probabilities p_K and p_L [see Equation (3.11) or Equation (3.12)]. These data are not known for the ITR converters, and therefore, must be treated as parameters in this study. Assuming that idling in an ITR converter appears only for a short time, idling failures can be neglected in the power calculation for this design. The probability of a certain number of failures occurring in the ITR network can, therefore, be calculated with the simple Newtonian formula of Equation (3.1), with $p = p_K + p_L = p_A$. It is shown in Figure 4.7 for some values of the parameter p_A.

In previous discussions on the ITR project, an electrical power of some 20 kW was taken as a realistic value. On the basis of the calculated converter characteristics for a cesium pressure of 6.6 Torr (Figure 2.4), this power can be realized for the following operating data for the intact network: / 55

Terminal voltage	$V = 10$ volts
Voltage of each converter	$u = 0.48$ volts
Current density in the electrode gap	$j = 10$ A/cm^2
Average heat source density in the emitter body	$= 121$ W/cm^3
Temperature at the hottest point of the emitter	$T_{E\ max} = 1{,}860$ °K

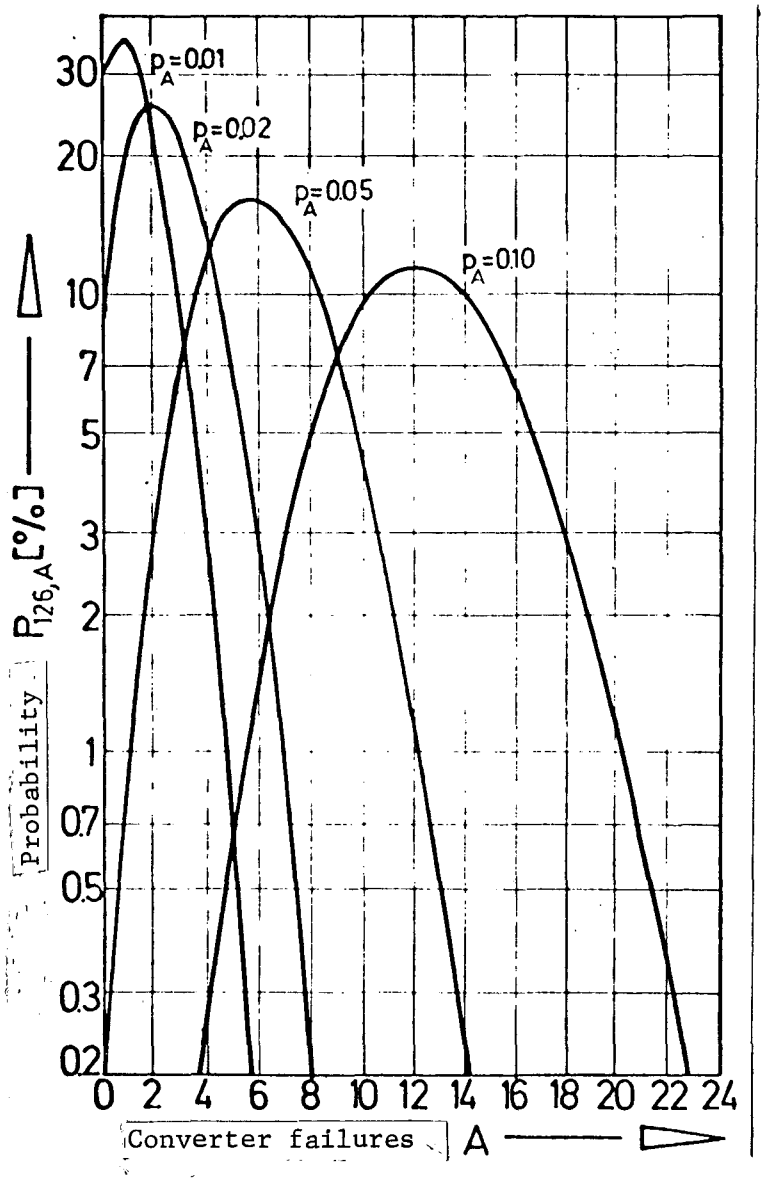

Figure 4.7: Probability of converter failures in an ITR network.

4.3.2 Heat source density required to maintain the rated electrical power with converter failures

When converters fail, the operating data listed above are, in general, changed. But by appropriate control of the thermal power of the reactor it is possible to hold the electrical power and the terminal voltage of the network constant. In the following, the change needed for the heat source density in the emitter body for compensation of failures will be shown. The emitter temperatures which occur will also be studied, as these can under some circumstances greatly impair the lifetimes of the converters. Such reactions are not considered here, however.

In spite of the simplifying assumption that a certain network power can be assigned to each number of converter failures (see Section 3.4.4), determination of the necessary heat source density in the emitter body requires some network calculations, as the ZUTIR computer program requires specification of the characteristics (and, therefore, of the heat source densities). Thus, for example, on the basis of the characteristic with the heat source density $\overline{\omega}| = 130\ W/cm^3$, the network has a power of 20.55 kW with eight failures, while ten failures / 56 correspond to a power of 19.85 kW.

Other positions with equally many failures have, in general, different network powers as their results.

The curve shown in Figure 4.8 represents one of the possible relations between the number of failures in an ITR network and the heat source density needed to maintain the rated power. It is used for the conclusions drawn in this section as representative of the ambiguous relation $\overline{\omega}|(A)$. An exact determination of this dependence is not very practical at the present state of knowledge about the converters planned for the ITR design (characteristics, failure probability).

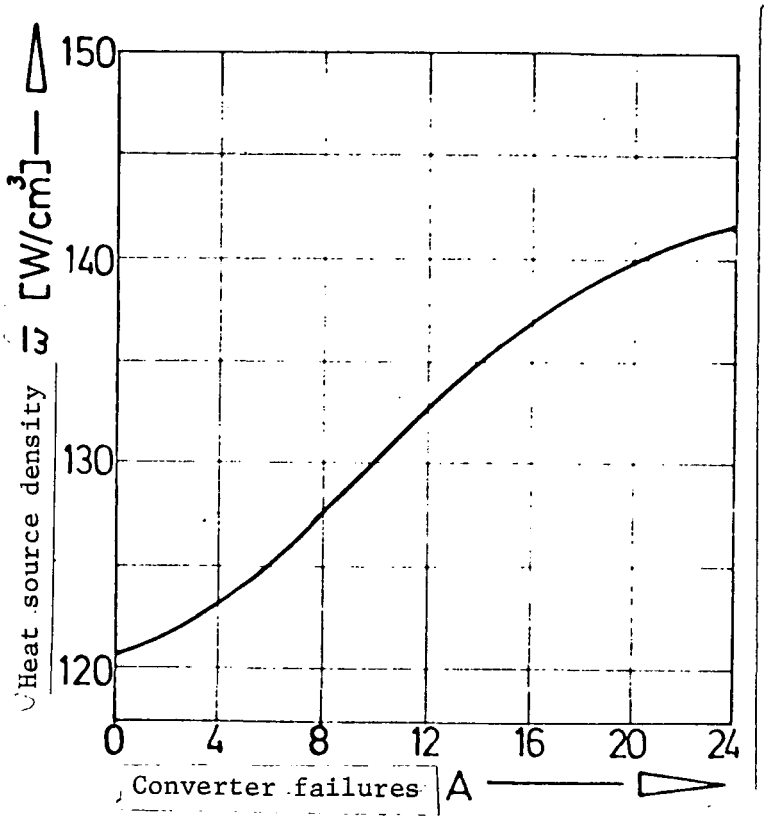

Figure 4.8: Heat source density required in the emitter bodies to maintain the rated power of an ITR network, as a function of the number of failures.

The excessive temperatures that appear with an idling converter were mentioned in Section 4.2.2. Haug (1969) has determined a value of about 170 W/cm^3 as the limit for the mean heat source density in emitter bodies of an ITR converter. If this is exceeded, unacceptable temperatures will occur in case of idling. From Figure 4.8 it can be seen that this power density is required to maintain the 20 kW rated power of the ITR only with very many failures.

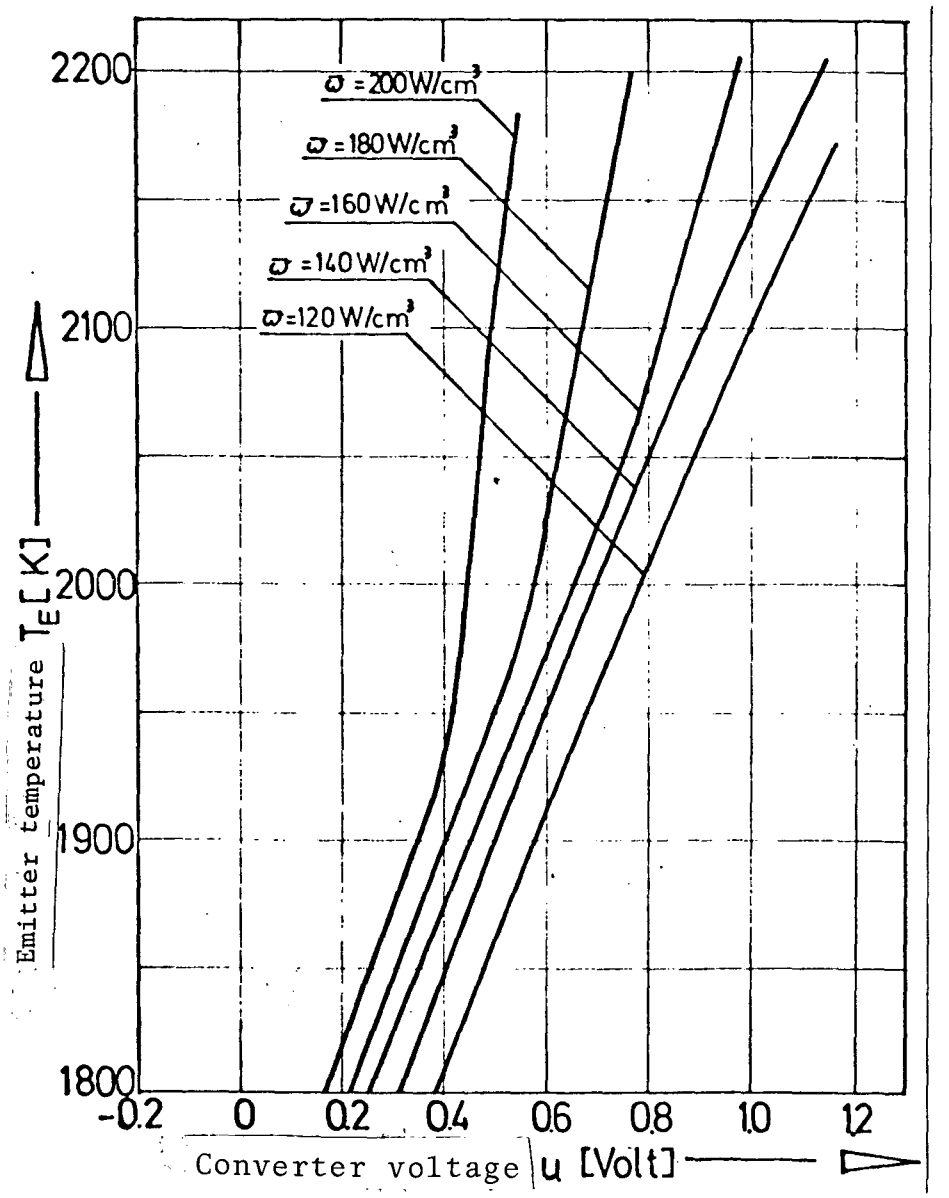

Figure 4.9: Dependence of the emitter temperature on the voltage and the heat source density.

4.3.3 Distribution of emitter temperatures

When converters in a network fail, the working points of the other converters are shifted (see Section 3.2). The emitter temperatures of the converters of the ITR network (Figure 4.9) are changed in this way, as not only the electron cooling but also the necessary heat source density in the fuel are affected by the failures. In the rows of the network in which there is a failure, the converters work at lower voltages than in the intact case. This results in lower emitter temperatures. In contrast, higher converter voltages are necessary in the other rows of the network in order to maintain the rated voltage of 10 Volts. Table 4.1 shows the distribution of emitter temperatures occurring as a result of this behavior.

/ 59

TABLE 4.1: NUMBER OF INTACT CONVERTERS HAVING EMITTER TEMPERATURES BETWEEN THE SPECIFIED LIMITS FOR THE NOMINAL DATA (N_{el} = 20 kW, V = 10 volts) AND THE GIVEN NUMBER OF CONVERTER FAILURES

Number of failures		6	10	14
Heat source density needed (W/cm^3)		125	130	135
Temperature intervals (°K)	1600-1650	0	1	1
	1650-1700	0	1	1
	1700-1750	4	3	8
	1750-1800	5	7	6
	1800-1850	16	7	6
	1850-1900	77	16	13
	1900-1950	14	66	40
	1950-2000	4	8	29
	2000-2050	0	2	7
	2050-2100	0	0	1

The table shows that the emitter temperatures generally increase with an increasing number of failures. It is significant that the number of converters for which the emitter temperature exceeds 2,000 °K increases, as a serious injury to the converter lifetime is to be feared at this temperature. Figure 4.10 shows the number of converters having emitter temperatures which exceed a specified temperature T' with randomly selected failure combinations.

/ 60

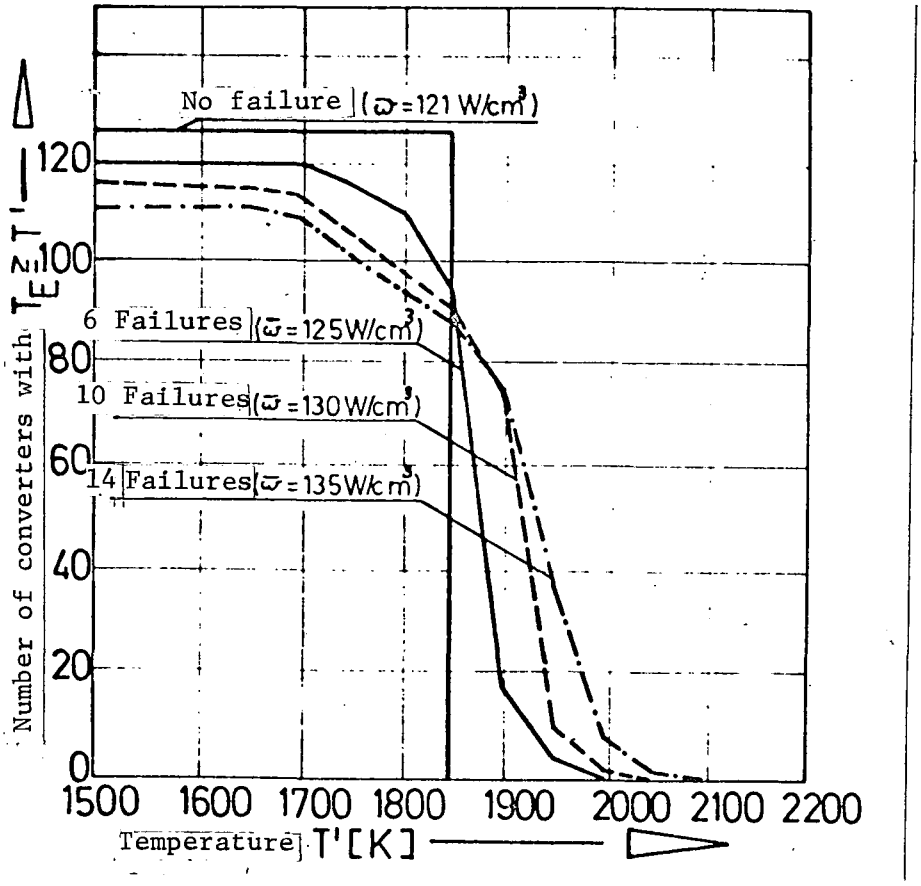

Figure 4.10: Number of converters having emitter temperatures above a certain value.

4.3.4. Probability of a certain operating condition

Because of the statistical nature of converter failures, we can only state a probability for a certain operating condition of a thermionic reactor (heat source density, emitter temperature) at the end of its planned operating time, even if the failure probability of a converter is known. In general, the operator of such a system will be particularly interested in how large the probability is that the conditions occurring (e. g., heat source density 170 W/cm^3) will be such that he can guarantee no satisfactory operation of the system. /| 61
Should the probability of occurrence of such critical conditions prove too large in the preliminary studies of a thermionic reactor, greater redundancy must be planned for under certain circumstances.

Figure 4.7 shows the probability of converter failures in an ITR network. The corresponding heat source density needed to compensate for these failures can be found in Figure 4.8. In this way it is possible to state the probability that a certain heat source density in the emitter body will not be exceeded. This is equal to the sum of the probabilities for all the failure combinations which require a smaller heat source density than that of interest (Figure 4.11). For instance, if the converters have a failure probability P_A (see Section 4.3.1) of 0.05, then there is a 99.98% probability that a heat source density of 135 W/cm^3 will not be exceeded in the course of operating the system.

Figure 4.12 shows, in a similar way, the probability that specified emitter temperatures will be exceeded in more than a prescribed number of converters. These results are also based on a single converter failure probability of 0.05. The intersection of the curves for 1,900 °K and 1,950 °K with the ordinate axis gives the probability that no failure will be present at the end of the system operating time (see Figure 4.7), as these

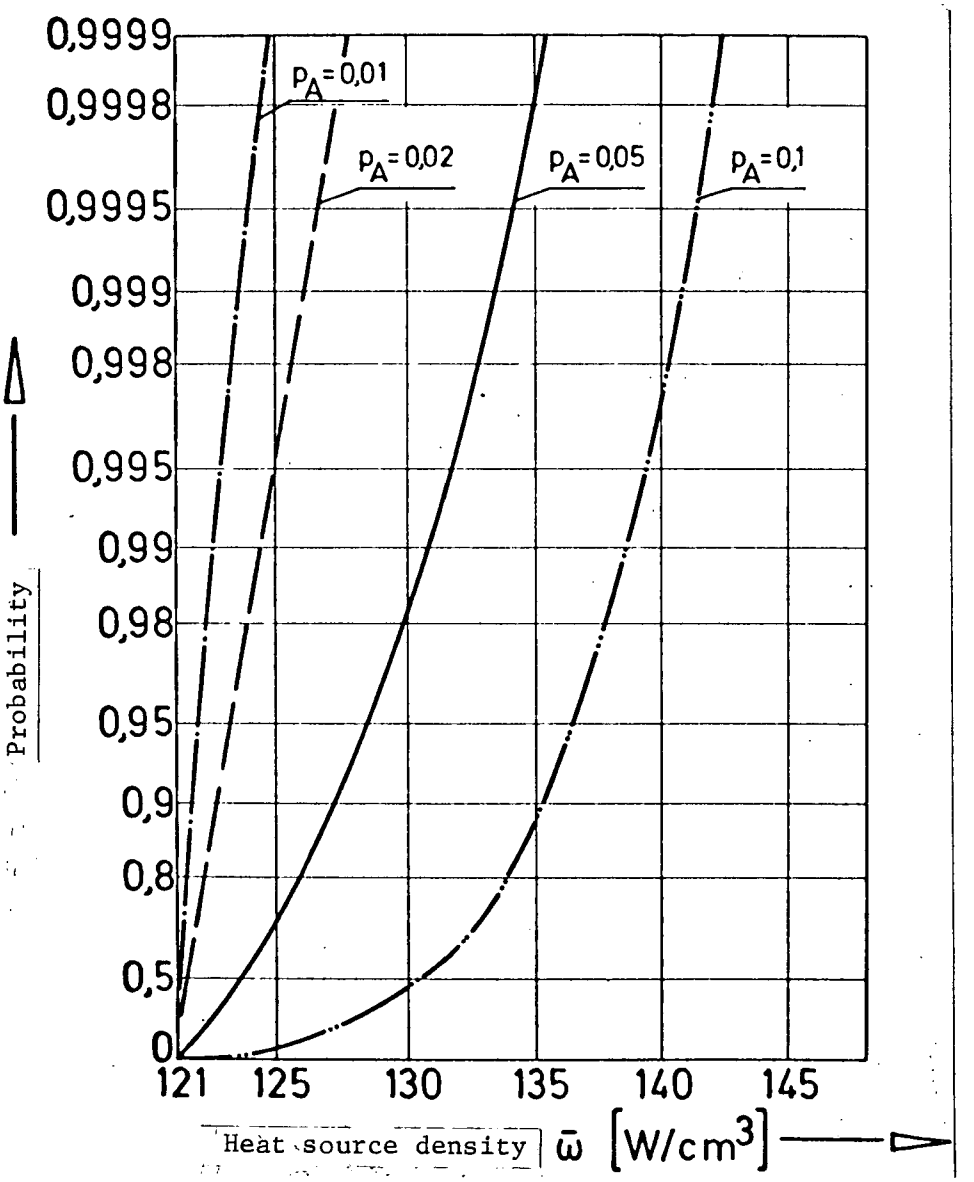

Figure 4.11: Probability that specified heat source densities in the emitter bodies of the ITR converters will not have to be exceeded in the course of operating the system.

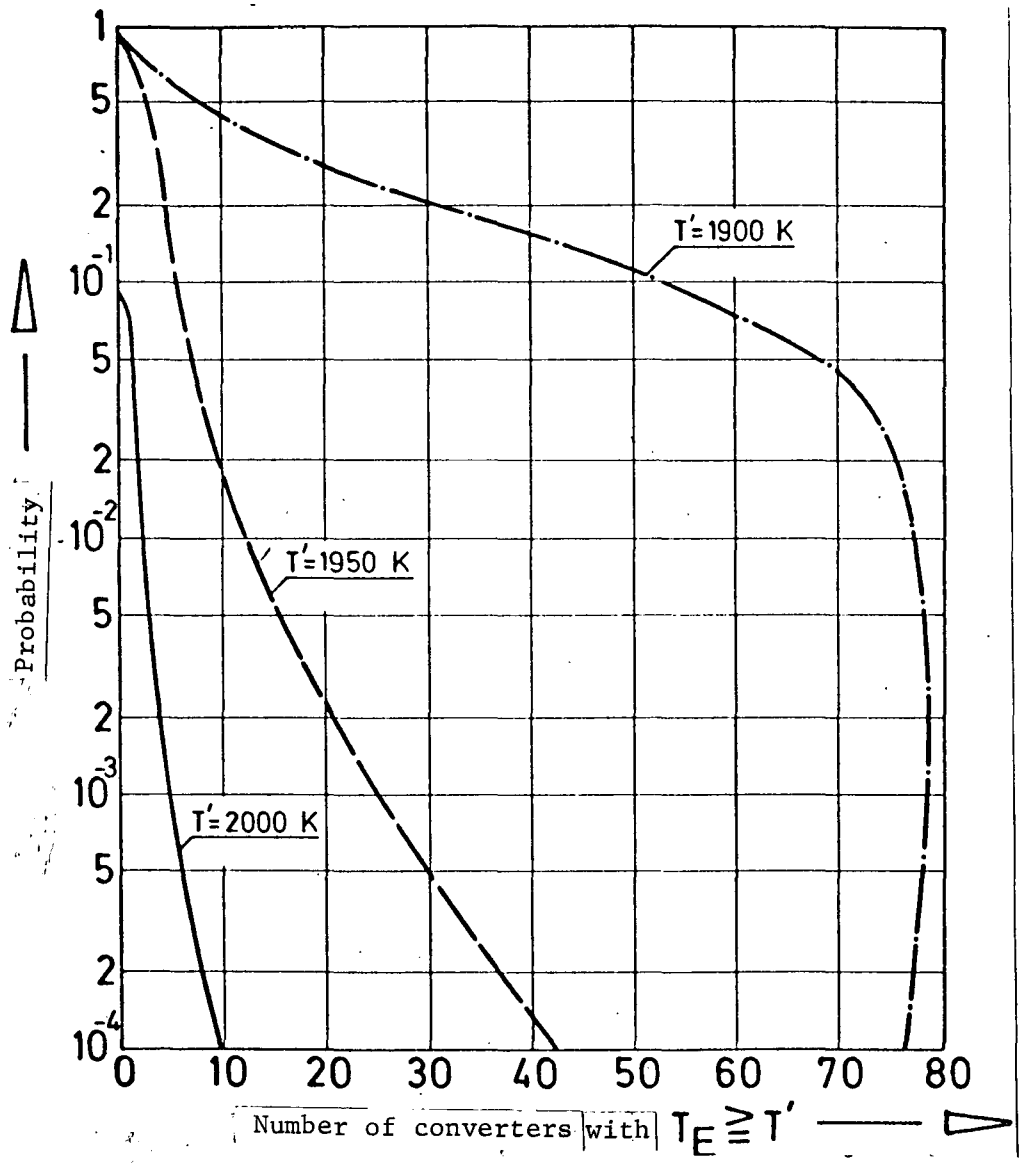

Figure 4.12: Probability of exceeding certain emitter temperatures.

temperatures are already exceeded in the neighborhood of the first failure.

With an increasing number of failures (negative direction of the ordinate in Figure 4.13), the number of converters with / 63 high emitter temperatures first increases. But since all the converters of a row in which there is a failure can generate only low voltages, they are relatively well-cooled, so that their emitter temperatures decrease. It is understandable, therefore, that the number of overheated converters decreases again for very many failures, as can be seen from Figure 4.12 (T' = 1,900 °K). The most inportant results from this figure are that there is only a probability of about 10% for the occurrence of emitter temperatures above 2,000°K, and most of the converters exhibit emitter temperatures less than 1,950°K.

5. CONCLUSIONS / 65

In this work it was shown, with the partially thermionic ITR reactor as an example, that in general converter failures require an increase in the power level of a thermionic reactor during its operation. In this, it was assumed that this reactor system is to furnish 20 kW of electrical power at a terminal voltage of 10 volts for a definite operating time. These values are maintained by the intact network with a mean heat source density in the emitter bodies of about 121 W/cm^3, with the emitter temperature about 1,860 °K. At the end of the operating period, in comparison, there is a 2% probability that the heat source density will have been increased above 130 W/cm^3 to maintain the rated data, if each converter has a 95% probability of remaining intact over the planned operating time.

The emitter temperatures of the intact converters are strongly affected by converter failures and the related increase of the heat source density. For converters connected in parallel,

the emitter temperature drops adjacent to a failed converter. Of greater importance, however, is the fact that the emitter temperature is sharply increased in the series-connected neighboring units. Under the assumptions stated above, then, there is a probability of about 10% for appearance of an ITR emitter temperature above 2,000 °K.

The emitter temperature affects the lifetime of the converter. Thus, if a considerable increase of emitter temperature occurs in a certain converter during its operation, its probability of failure is increased. Such feed-back effects are neglected, however, in this work. A type of Monte Carlo computation is necessary for the strict treatment of this problem, in which chains of failures are followed over the / 66
operating time and their statistically weighted results are combined into a total result.

In spite of the assumption used in this work, that all converters have a uniform probability of failure, some interesting conclusions can be drawn from its results for the design of thermionic reactors. Thus, the maximum power of the individual converters of an incore thermionic reactor may be used as the basis for determining the potential rated power only in the case of a very brief operating time. For longer operating life, we must take converter failures into account. Either directly or through the temperature increase in the other converters, they force the system to produce less power than that initially possible. For the converters of the ITR network, Haug (1968) has calculated an electrical power density of about 8 W/cm^2, referred to the emitter area, at an emitter temperature of 2,000 °K. This power density would correspond to a total power of about 32 kW for the converter network. On the basis of a failure probability of 5% for a converter, 5 W/cm^2 appears to be the limit of power density which should not be exceeded at the beginning of operation of the system because of the high emitter temperatures

resulting and the related danger of a considerably diminished lifetime for the converters concerned.

These considerations apply in principle for all thermionic reactors with converters lacking thermal interaction with the emitter temperatures. On the other hand, thermionic reactors with thermal coupling, which prevents great differences in the emitter temperatures of the individual converters, can be designed for a considerably higher proportion of the potential power of the intact network [see Dagbjartsson (1968) and Abbate (1968)]. However, we cannot obtain a quantitative prediction of the network data for such a concept until after a general experimental determination of the characteristics with the methods described in this work.

This study was performed at the Institute for Nuclear Energetics of the University, Stuttgart.

I thank Prof. Dr. K. H. Höcker for his kind support.

I thank Dr.-Ing. E. Wolf and Dipl.-Phys. D. Lutz for fruitful and clarifying discussions.

REFERENCES

1. Budnick, D. Incore-Thermionik-Reaktor mit radialer Treiberzone und flacher Leistungsdichtverteilung in der Thermionikzone (Incore Thermionic Reactor with Radial Driver Zone and Flat Power Density Distribution in the Thermionic Zone). Dissertation, University, Stuttgart, 1968. /69

2. Dagbjartsson, S., M. Groll, O. Schlörb and R. Pruschek. An Improved Out-of-Core-Thermionic Reactor for Low Power. Thermionic Conversion Specialist Conference, Boston 1968, Conference Record, p. 299.

3. Diakov, B. B. Failure Models and Reliability Analysis of Thermionic Converter Component Part. Proc. 2nd Int. Conference on Thermionic Electrical Power Generation Stresa, 1968, Paper F-10.

4. Gammel, G., M. F. Koskinen and A. de Troyer. On the Development of a Thermionic Generator Heated with Actinium 227. Raumfahrtforschung, Vol. 13, 1969, p. 1.

5. Groll, M. On the Design of Radiators for Spacecraft. Atomkernenergie, Vol. 9, No. 10, 1965, p. 353.

6. Haug, W. Grenzleistung einer Incore-Thermionikzelle (Limiting Power of an Incore Thermionic Reactor). Dissertation, University, Stuttgart, 1969.

7. Höcker, K. H. and Mitarbeiter. Special Number on Nuclear Energy. Thermionikreaktoren, Vol. 9, No. 10, 1965.

8. Holland, J. W. Energy Transfer Measurements and Correlation on a Cesium Thermionic Converter. Thermionic Conversion Specialist Conference Gatlinburg, 1963, Conference Record, p. 8.

9. Homeyer, W. G., C. A. Heath and A. J. Gietzen. Thermionic Reactors for Electrical Propulsion-Parametric Studies. Proc. 2nd Int. Conference on Thermionic Electrical Power Generation, Stresa, 1968, Paper B-5. /70

10. van Homissen, J. E. and D. E. Holtschlag. In-Reactor Thermionic Converter Testing Experience at General Electric. Proc. 2nd Int. Conference on Thermionic Power Generation, Stresa, 1968, Paper C-1.

11. Howard, R. C. and J. B. Dunlay. Converter SD-4 Design and Summary of Test Results. Energy Conversion, Vol. 1, 1969, p. 25.

12. Jester, A., F. Gross, H. Holick and C. A. Busse. A Nuclear Heated Thermionic Converter. Thermionic Conversion Specialist Conference, Houston, 1966, Conference Record, p. 419.

13. Kitrilakis, S. and P. Brpsens. Experimental Correlation of Electron Emission Cooling and Optimum Collector Temperature. Thermionic Conversion Specialist Conference, San Diego, 1965, Conference Record, p. 316.

14. Kondratiev, F. V. and G. V. Sinyutin. Experimental Verification on the Rasor Phenomenological Theora of the Arc Mode Regime of a Cesium Thermionic Converter. Proc. 2nd Int. Conference on Thermionic Electrical Power Generation, Stresa 1968, Paper H-6.

15. Lindner, A. Statistische Methoden (Statistical Methods). Biskhauser Verlag, Basel and Stuttgart, 1964.

16. Merra, S. G. and J. H. Weinstein. Recent Process in the Development of Solar Thermionic Converter. Thermionic Conversion Specialist Conference, Gatlinburg, 1963, Conference Record, p. 295.

17. Pruschek, R., S. Dagbjartsson, D. Emendörfer, M. Groll, W. Haug, B. Rörborn, H. Unger and E. Wolf. Results of Studies on Various Fast and Thermal Thermionic Reactor Systems. Proc. 2nd Int. Conference on Thermionic Electrical Power Generation, Stresa, 1968, Paper B-2. /71

18. Rasor, N. S. Analytical Description of Cesium Diode Phenomenology. Proc. 1st Int. Conference on Thermionic Electrical Power Generation, London, 1968.

19. Rufeh, F., D. Lieb and L. van Someren. Summary of Applied Research Program in Thermionic Conversion During Recent Years. Proc. 2nd Int. Conference on Thermionic Electrical Power Generation, Stresa, 1968, Paper A-1.

20. Schock, A. and M. J. Abbate. Comparison of Methods for Calculating Radiative Heat Transfer. Proc. 2nd Int. Conference on Thermionic Electrical Power Generation, Stresa, 1968, Paper F-3.

21. Schubert, K. P. Entwurfsstudie über konstruktive Möglichkeiten zur Parallelschaltung von Thermionikzellen in einem Incore-Thermionikreaktors (Developmental Studies on the Possibilities of Designing for Parallel Connection of Thermionic Cells in an Incore Thermionic Reactor). Report

of the Institute for Nuclear Energetics, Stuttgart, No. 5-61e, 1968.

22. Wolf, E. Optimierung des Brennelements eines Incore-Thermionickreaktors (Optimization of the Fuel Element of an Incore Thermionic Reactor). Dissertation, University, Stuttgart, 1968.

23. Yates, M. K. and G. O. Fitzpatrick. Cesium Sorption in Materials for Thermionic Converters. Gulf General Atomic Report GA 8574, 1968.

24. Abbate, M. J., C. L. Eisen, B. Raab and A. Schock. External Fuel Thermionic Reactors. Proceedings on the 2nd Int. Conference on Thermionic Electrical Power Generation, Stresa, 1968, Paper B-6.

Translated for National Aeronautics and Space Administration under Contract No. NASw 2035, by SCITRAN, P. O. Box 5456, Santa Barbara, California, 93108